Noisy random resistor networks: Renormalized field theory for the multifractal moments of the current distribution

Olaf Stenull and Hans-Karl Janssen
Institut für Theoretische Physik III, Heinrich-Heine-Universität, Universitätsstraße 1, 40225 Düsseldorf, Germany
(Received 13 July 2000; published 15 February 2001)

We study the multifractal moments of the current distribution in randomly diluted resistor networks near the percolation threshold. When an external current is applied between two terminals x and x' of the network, the lth multifractal moment scales as $M_l^{(l)}(x,x') \sim |x-x'|^{\psi_l/\nu}$, where ν is the correlation length exponent of the isotropic percolation universality class. By applying our concept of master operators [Europhys. Lett. **51**, 539 (2000)] we calculate the family of multifractal exponents $\{\psi_l\}$ for $l \geqslant 0$ to two-loop order. We find that our result is in good agreement with numerical data for three dimensions.

DOI: 10.1103/PhysRevE.63.036103 PACS number(s): 64.60.Ak, 05.40.−a, 72.70.+m

I. INTRODUCTION

Percolation [1] is a leading paradigm for disorder. It provides an intuitively appealing and transparent model of the irregular geometry that occurs in disordered systems. Moreover, it is a prototype of a phase transition. Although percolation represents the simplest model of a disordered system, it has many applications, e.g., polymerization, porous and amorphous materials, thin films, spreading of epidemics, etc.

In particular the transport properties of percolation clusters have gained a vast amount of interest over recent decades. Random resistor networks (RRN's) are a prominent model for transport on percolation clusters. By means of RRN's one can study the conductivity of disordered media, which might be important for technical applications. Nonlinear random resistor networks, for which the voltage drop over an individual resistor depends on some power of the current flowing through it, can be exploited to derive various fractal dimensions of percolation clusters. From the conceptual point of view, RRN's have the advantage that one can formulate a field theoretic Hamiltonian amenable to renormalization group analysis. Via RRN's one can learn about diffusion on disordered substrates, since the diffusion constant D and the conductivity Σ of the system are related by the Einstein relation

$$\Sigma = \frac{e^2 n}{K_B T} D, \tag{1.1}$$

where e and n denote the charge and the density of the mobile particles. The connection of the two problems is particularly important, since up to date no direct approach to diffusion on percolation clusters by means of a dynamic field theory exists.

In this paper we study the distribution of currents in RRN's. The current distribution has many interesting features, one of which is multifractality [2]. This means that the distribution is not controlled by one or two relevant length scales, but rather by an infinite hierarchy of such length scales. The concept of multifractality was introduced for turbulence [3]. It has been applied successfully in diverse areas including diffusion near fractals [4], electrons in disordered media [5], polymers in disordered media [6], random ferromagnets [7], chaotic dissipative systems [8], and heartbeat [9].

Due to the multifractality infinitely many exponents are needed to characterize the current distribution. Consider two connected terminals x and x' of the network. Suppose a current I is inserted at x and withdrawn at x'. The lth moment of the current distribution, given (apart from technical details, cf. Sec. II C) by

$$M_l^{(l)}(x,x') = \left\langle \sum_b i_b^{2l} \right\rangle_C, \tag{1.2}$$

where the sum runs over all current carrying bonds (the backbone), $\langle \cdots \rangle_C$ stands for the average over all diluted configurations, and i_b is an abbreviation for I_b/I, scales at criticality as [11]

$$M_l^{(l)}(x,x') \sim |x-x'|^{-x_l}. \tag{1.3}$$

The x_l constitute an infinite set of exponents which are not related to each other in a linear fashion, i.e., the multifractal moments do not show the usual gap scaling commonly encountered in critical phenomena.

Each of the $M_l^{(l)}$ is associated with a particular subset of backbone bonds having its distinct fractal dimension. Let $n(i)$ be the number of bonds carrying current i. Upon applying the saddle point method one finds that the main contribution to the lth moment is given by [10]

$$n(i_l) \sim |x-x'|^{f(l)}, \tag{1.4}$$

with the multifractal spectrum $f(l)$ and the multifractal exponents x_l being related to each other by a Legendre transformation. $f(l)$ can be interpreted as the fractal dimension of the subset of bonds dominating $M_l^{(l)}$.

An elegant approach for studying the multifractal moments is to consider RRN's with microscopic noise, i.e., random networks in which the conductances of the individual resistors fluctuate about some mean. These noisy RRN's were originally introduced by Rammal *et al.* [11] to study the effects of flicker $(1/f)$ noise. Flicker noise refers to the low frequency spectrum of excess voltage fluctuations measured when a constant current is applied to a resistor. The lth noise

 ©2001 The American Physical Society

cumulant $C_R^{(l)}(x,x')$ of the total resistance between the terminals x and x' is proportional to $M_I^{(l)}(x,x')$ by virtue of Cohn's theorem [12].

Historically, the existence of the set of multifractal exponents $\{x_l\}$ was proposed by Rammal *et al.* [11]. The authors determined several of their exponents for two dimension by numerical simulations. A set of exponents $\{\zeta_{2l}\}$ equivalent to $\{-x_l\nu\}$, where ν is the correlation length exponent for percolation, was also proposed by de Arcangelis *et al.* [13]. These authors derived their exponents for several hierarchical structures analytically. The field theoretic description of multifractality in RRN's was pioneered by Park, Harris, and Lubensky (PHL) [14]. Based on an approach by Stephen [15] they formulated a $(D\times E)$-fold replicated Hamiltonian for noisy RRN's. The contributions to the Hamiltonian leading to multifractal behavior contain powers of replica space gradients analogous to powers of real space gradients, which were accounted for as an origin of multifractality by Duplantier and Ludwig [16]. PHL introduced a set of exponents $\{\psi_n\}$ identical to the set $\{-x_n\nu\}$ and calculated it to first order in $\epsilon=6-d$, where d denotes the spatial dimension. Later on Fourcade and Tremblay [17] gave a reinterpretation of the work by PHL. Batrouni *et al.* [18] computed several multifractal exponents for $d=3$ by numerically solving Kirchhoff's equations. Recently Barthélémy *et al.* [19] performed simulations indicating that in the thermodynamic limit the $M_I^{(l)}$ do not exist for $l<0$.

In this article we study the moments of the current distribution by renormalized field theory. We extend our real world interpretation of Feynman diagrams [20–22] to RRN's with noise. Upon introducing multifractal moments for Feynman diagrams we reformulate the field theory of PHL in a way that to our opinion is less complex and more intuitive. By carefully analyzing the relevance of the field theoretic operators related to the noise cumulants, we show that the multifractality is associated with dangerously irrelevant master operators [23]. We calculate the set $\{\psi_l\}$ for $l\geqslant 0$ to second order in ϵ. Finally, we compare our result to numerical simulations.

II. THE MODEL

This section provides background on noisy RRN's. It is guided by the work of Stephen [15] and PHL [14].

A. Random resistor networks

Consider a d-dimensional lattice, where bonds between nearest neighboring sites i and j are randomly occupied with probability p or empty with probability $1-p$. Each occupied bond $\langle i,j\rangle$ has a conductance $\sigma_{i,j}$. Unoccupied bonds have conductance zero. The bonds obey Ohm's law

$$\sigma_{i,j}(V_j-V_i)=I_{i,j}, \tag{2.1}$$

where $I_{i,j}$ is the current flowing through the bond from j to i and V_i is the potential at site i.

Suppose a current I is injected into a cluster at site x and withdrawn at site x'. The union of all sites belonging to all self-avoiding paths between x and x' is referred to as the backbone between x and x'. The power dissipated on the backbone is by definition

$$P=I(V_x-V_{x'}). \tag{2.2}$$

Using Ohm's law, it may be expressed entirely in terms of voltages as

$$P=R(x,x')^{-1}(V_x-V_{x'})^2=\sum_{\langle i,j\rangle}\sigma_{i,j}(V_i-V_j)^2=P(\{V\}). \tag{2.3}$$

Here $R(x,x')$ is the total resistance of the backbone, the sum is taken over all nearest neighbor pairs on the cluster, and $\{V\}$ denotes the corresponding set of voltages. As a consequence of the variation principle

$$\frac{\partial}{\partial V_i}\left[\frac{1}{2}P(\{V\})-\sum_j I_jV_j\right]=0, \tag{2.4}$$

one obtains Kirchhoff's law

$$\sum_{\langle j\rangle}\sigma_{i,j}(V_i-V_j)=-\sum_{\langle j\rangle}I_{i,j}=I_i, \tag{2.5}$$

where $I_i=I(\delta_{i,x}-\delta_{i,x'})$ and the summations extend over the nearest neighbors of i.

Alternatively to Eq. (2.3) the power can by rewritten in terms of the currents as

$$P=R(x,x')I^2=\sum_b \rho_bI_b^2=P(\{I_b\}), \tag{2.6}$$

with $\{I_b\}$ denoting the set of currents flowing through the individual bonds, $b=\langle i,j\rangle$, and $\rho_b=\sigma_b^{-1}$. Obviously the cluster may contain closed loops as subnetworks. Suppose there are currents $\{I^{(\mathrm{loop})}\}$ circulating independently around a complete set of independent closed loops. Then the power is a function not only of I but also of the set of loop currents. The potential drop around closed loops is zero. This gives rise to the variation principle

$$\frac{\partial}{\partial I^{(\mathrm{loop})}}P(\{I^{(\mathrm{loop})}\},I)=0. \tag{2.7}$$

Equation (2.7) may be used to eliminate the loop currents and thus provides us with a method to determine the total resistance of the backbone via Eq. (2.6).

Since the resistance of the backbone depends on the configurations C of the randomly occupied bonds, one introduces an average $\langle\cdots\rangle_C$ over these configurations. It is important to recognize that the resistance between disconnected sites is infinite. Therefore one considers only those sites x and x' known to be on the same cluster. In practice this is done by introducing the indicator function $\chi(x,x')$ which, for a given configuration C, is unity if x and x' are connected and zero otherwise. Then the lth moment of the resistance R with respect to the average $\langle\cdots\rangle_C$ subject to x and x' being on the same cluster is given by

$$\langle\chi(x,x')R(x,x')^l\rangle_C/\langle\chi(x,x')\rangle_C. \tag{2.8}$$

B. Noise in random resistor networks

In the following we consider RRN's with noise in the sense that the conductances σ_b of occupied bonds fluctuate about some mean. To be specific, the σ_b are equally and independently distributed random variables with mean $\overline{\sigma}$ and higher cumulants $\Delta^{(l\geqslant 2)}$. The distribution function f might, for example, be Gaussian. Nevertheless, our considerations are not limited to this particular choice. In order to suppress unphysical negative conductances, the assumption $\Delta^{(l)} \ll \overline{\sigma}^l$ is made. In general the backbone resistance will depend on the set of conductances of occupied bonds $\{\sigma_b\}$. Its noise average will be denoted by

$$\{R(x,x')\}_f = \int \prod_b d\sigma_b f(\sigma_b) R(x,x') \tag{2.9}$$

and the corresponding cumulants by

$$\{R(x,x')^l\}_f^{(c)} = \frac{\partial^l}{\partial \lambda^l} \ln\{\exp[\lambda R(x,x')]\}_f|_{\lambda=0}. \tag{2.10}$$

Both kinds of disorder, the random dilution of the lattice and the fluctuation of the bond conductances about their mean $\overline{\sigma}$, influence the statistical properties of the backbone resistance. They are reflected by the moments

$$M_R^{(l)}(x,x') = \langle \chi(x,x')\{R(x,x')^l\}_f \rangle_C / \langle \chi(x,x') \rangle_C \tag{2.11}$$

and the cumulants

$$C_R^{(l)}(x,x') = \langle \chi(x,x')\{R(x,x')^l\}_f^{(c)} \rangle_C / \langle \chi(x,x') \rangle_C. \tag{2.12}$$

C. Moments of the current distribution

The noise cumulants $C_R^{(l)}$ characterize the distribution of currents flowing through the network. This section provides a relation between the $C_R^{(l)}$ and the moments of the current distribution.

Equation (2.9) defines the noise average as an average with respect to the distribution of the bond conductances σ_b. Equally well one might express the backbone resistance in terms of the bond resistances and average over the distribution of the ρ_b. Since the σ_b are independently and equally distributed, the ρ_b are distributed by the same means. Assume that the distribution function of the deviations $\delta\rho_b = \rho_b - \overline{\rho}$ of the resistance of each bond from its average $\overline{\rho}$ has the form

$$g_s(\delta\rho_b) = \frac{1}{s} h\left(\frac{\delta\rho_b}{s}\right) \tag{2.13}$$

and that

$$\lim_{s\to 0} g_s(\delta\rho_b) = \delta(\delta\rho_b). \tag{2.14}$$

s is a variable with units of resistance that sets the scale of the distribution. With this form of g_s, the nth cumulant v_n of $\delta\rho_b$ tends to zero as s^n. This follows from the generating function $c(\lambda s)$ of the v_n:

$$\exp[c(\lambda s)] = \{\exp(\lambda\,\delta\rho_b)\}_f = \int dy\, h(y) \exp(\lambda s y) = \exp\left(\sum_{n=1}^{\infty} \frac{\lambda^n}{n!} v_n\right), \tag{2.15}$$

where $v_n = c_n s^n$ with c_n being constants. In general $\{R(x,x')^l\}_f^{(c)}$ depends on the entire set of cumulants $\{v_n\}$. However, in the limit $s\to 0$ the leading term is proportional to v_l as we will see immediately. Consider the generating function $C(\lambda)$ of the cumulants $\{R(x,x')^l\}_f^{(c)}$,

$$\exp[C(\lambda)] = \int \prod_b d\,\delta\rho_b\, g_s(\delta\rho_b) \exp[\lambda R(x,x')]. \tag{2.16}$$

Expansion of the backbone resistance in a power series in the $\delta\rho_b$ leads to

$$\exp[C(\lambda)] = \int \prod_b dy_b\, h(y_b) \exp\left[\lambda R^0(x,x') + \lambda \sum_{k=1}^{\infty} \sum_{b_1,\ldots,b_k} \frac{s^k}{k!} \frac{\partial^k R(x,x')}{\partial\rho_{b_1}\cdots\partial\rho_{b_k}}\bigg|_{\overline{\rho}} y_{b_1}\cdots y_{b_k}\right], \tag{2.17}$$

where $R^0(x,x')$ is the resistance when $\delta\rho_b = 0$ for every bond b. Equation (2.17) can be rearranged as

$$\begin{aligned}
\exp[C(\lambda)] &= \exp\left[\lambda R^0(x,x') + \lambda \sum_{k=2}^{\infty} \sum_{b_1,\ldots,b_k} \frac{s^k}{k!} \frac{\partial^k R(x,x')}{\partial\rho_{b_1}\cdots\partial\rho_{b_k}}\bigg|_{\overline{\rho}} \times \frac{\partial^k}{\partial z_{b_1}\cdots\partial z_{b_k}} \prod_b \exp[c(z_b)]\bigg|_{\lambda s \Sigma_b [\partial R(x,x')/\partial\rho_b]|_{\overline{\rho}}}\right] \\
&= \exp\left[\lambda R^0(x,x') + \sum_{l=1}^{\infty} (\lambda s)^l c_l \sum_b \left(\frac{\partial R(x,x')}{\partial\rho_b}\bigg|_{\overline{\rho}}\right)^l + \sum_{i=2}^{\infty} f_i(\lambda s^i)\right],
\end{aligned} \tag{2.18}$$

where f_i are functions of λs^i. Hence, for $l \geqslant 2$,

$$\{R(x,x')^l\}_f^{(c)} = c_l \sum_b \left(s \frac{\partial R(x,x')}{\partial\rho_b}\bigg|_{\overline{\rho}}\right)^l [1 + O(s)]. \tag{2.19}$$

In the limit $s\to 0$ the leading term is

$$\{R(x,x')^l\}_f^{(c)} = v_l \sum_b \left(\frac{\partial R(x,x')}{\partial\rho_b}\bigg|_{\overline{\rho}}\right)^l = v_l \sum_b \left(\frac{I_b}{I}\right)^{2l}, \tag{2.20}$$

where we have used Cohn's theorem Eq. (A5). Upon substitution of Eq. (2.20) into Eq. (2.12) one finds for the noise cumulants

$$C_R^{(l)}(x,x') = v_l M_I^{(l)}(x,x'), \tag{2.21}$$

i.e., the noise cumulant $C_R^{(l)}$ is proportional to the lth multifractal moment

$$M_I^{(l)}(x,x') = \left\langle \chi(x,x') \sum_b \left(\frac{I_b}{I}\right)^{2l} \right\rangle_C \Big/ \langle \chi(x,x') \rangle_C \tag{2.22}$$

of the current distribution.

D. Generating function

Our aim is to determine $C_R^{(l)}$. Hence the task is to solve the set of Kirchhoff's equations (2.5) and to perform the averages over the diluted lattice configurations and the noise. This can be achieved by employing the replica technique [15]. In order to treat the averages $\langle \cdots \rangle_C$ and $\{\cdots\}_f$ separately, PHL introduced $(D \times E)$-fold replicated voltages,

$$V_x \to \vec{\vec{V}}_x = \begin{pmatrix} V_x^{(1,1)} & \cdots & V_x^{(1,D)} \\ \vdots & \ddots & \vdots \\ V_x^{(E,1)} & \cdots & V_x^{(E,D)} \end{pmatrix}. \tag{2.23}$$

Note from the definitions Eq. (2.12) and Eq. (2.10) that one has to treat the two averages independently in the calculation of $C_R^{(n)}$. In contrast, for calculating $M_R^{(n)}$ it is not necessary to distinguish between the two averages because one could also introduce a composite distribution function

$$f^{\text{comp}}(\sigma) = (1-p)\,\delta(\sigma) + p f(\sigma) \tag{2.24}$$

and a single, say D-fold, replication would be sufficient.

To construct a generating function for the noise cumulants one introduces

$$\psi_{\vec{\vec{\lambda}}}(x) = \exp(i \vec{\vec{\lambda}} \cdot \vec{\vec{V}}_x), \tag{2.25}$$

where $\vec{\vec{\lambda}} \cdot \vec{\vec{V}}_x = \Sigma_{\alpha,\beta=1}^{D,E} \lambda^{(\alpha,\beta)} V_x^{(\alpha,\beta)}$ and $\vec{\vec{\lambda}} \neq \vec{\vec{0}}$. The corresponding correlation functions

$$G(x,x';\vec{\vec{\lambda}}) = \langle \psi_{\vec{\vec{\lambda}}}(x)\, \psi_{-\vec{\vec{\lambda}}}(x') \rangle_{\text{rep}} \tag{2.26}$$

are defined as

$$G(x,x';\vec{\vec{\lambda}}) = \lim_{D\to 0} \left\langle \left\{ \frac{1}{\prod_{\beta=1}^{E} Z(\{\sigma_b^{(\beta)}\},C)^D} \int \prod_j d\vec{\vec{V}}_j \times \exp\left[-\frac{1}{2} \sum_{\beta=1}^{E} P(\{\vec{V}^{(\beta)}\},\{\sigma_b^{(\beta)}\},C) + \frac{i\omega}{2} \sum_i \vec{\vec{V}}_i^2 + i\vec{\vec{\lambda}} \cdot (\vec{\vec{V}}_x - \vec{\vec{V}}_{x'}) \right] \right\}_f \right\rangle_C. \tag{2.27}$$

Here $d\vec{\vec{V}}_j = \Pi_{\alpha,\beta=1}^{D,E} dV_j^{(\alpha,\beta)}$,

$$P(\{\vec{V}^{(\beta)}\},\{\sigma_b^{(\beta)}\},C) = \sum_{\alpha=1}^{D} \sum_{\langle i,j \rangle} \sigma_{i,j}^{(\beta)} (V_i^{(\alpha,\beta)} - V_j^{(\alpha,\beta)})^2 \tag{2.28}$$

with $\vec{V}_x^{(\beta)} = (V_x^{(1,\beta)}, \ldots, V_x^{(D,\beta)})$, and Z is the normalization

$$Z(\{\sigma_b^{(\beta)}\},C) = \int \prod_j dV_j \times \exp\left[-\frac{1}{2} P(\{V\},\{\sigma_b^{(\beta)}\},C) + \frac{i\omega}{2} \sum_i V_i^2 \right]. \tag{2.29}$$

Note that we have introduced an additional power term $(i\omega/2)\Sigma_i V_i^2$. This is necessary to give the integrals in Eqs. (2.27) and (2.29) a well defined meaning. Without this term the integrands depend only on voltage differences and the integrals are divergent. Physically the new term corresponds to grounding each lattice site by a capacitor of unit capacity. The original situation may be restored by taking the limit of vanishing frequency, $\omega \to 0$.

The integrations in Eq. (2.27) can be carried out by employing the saddle point method. Since the integrations are Gaussian the saddle point method is exact in this case. The saddle point equation is identical to the variation principle stated in Eq. (2.4). Thus the maximum of the integrand is determined by the solution of Kirchhoff's equations (2.5) and

$$G(x,x';\vec{\vec{\lambda}}) = \left\langle \prod_{\beta=1}^{E} \left\{ \exp\left[-\frac{\vec{\lambda}^{(\beta)2}}{2} R^{(\beta)}(x,x') \right] \right\}_f \right\rangle_C. \tag{2.30}$$

The right hand side of Eq. (2.30) may be expanded in terms of the cumulants defined in Eq. (2.10). This gives

$$G(x,x';\vec{\vec{\lambda}}) = \left\langle \exp\left[\sum_{l=1}^{\infty} \frac{(-1/2)^l}{l!} K_l(\vec{\vec{\lambda}}) \{R(x,x')^l\}_f^{(c)} \right] \right\rangle_C, \tag{2.31}$$

where K_l is defined by

$$K_l(\vec{\vec{\lambda}}) = \sum_{\beta=1}^{E} \left[\sum_{\alpha=1}^{D} (\lambda^{(\alpha,\beta)})^2 \right]^l. \tag{2.32}$$

We learn that the correlation function G can be exploited as a generating function for the noise cumulants via

$$\langle \chi(x,x') \rangle_C C_R^{(n)}(x,x') = \frac{\partial}{\partial[(-1/2)^n (n!)^{-1} K_n(\vec{\vec{\lambda}})]} G(x,x';\vec{\vec{\lambda}})\big|_{\vec{\vec{\lambda}}=\vec{\vec{0}}}. \tag{2.33}$$

Note that $M_R^{(1)} = C_R^{(1)}$.

E. Field theoretic Hamiltonian

Since infinite voltage drops between different clusters may occur, it is not guaranteed that Z stays finite, i.e., the limit $\lim_{D\to 0} Z^{DE}$ is not well defined. Moreover, $\vec{\vec{\lambda}} = \vec{\vec{0}}$ has to be excluded properly. Both problems can be handled by resorting to a lattice regularization of the integrals in Eqs. (2.27) and (2.29). One switches to voltage variables $\vec{\vec{\theta}}$

$=\Delta\theta\vec{k}$ taking discrete values on a $(D\times E)$-dimensional torus, i.e., $\vec{k}$ is chosen to be a $(D\times E)$-dimensional integer with $-M<k^{(\alpha,\beta)}\leqslant M$ and $k^{(\alpha,\beta)}=k^{(\alpha,\beta)}\mathrm{mod}(2M)$. $\Delta\theta=\theta_M/M$ is the gap between successive voltages and θ_M is the voltage cutoff. The continuum may be restored by taking $\theta_M\to\infty$ and $\Delta\theta\to 0$. By setting $\theta_M=\theta_0 M$, $M=m^2$, and, respectively, $\Delta\theta=\theta_0/m$, the two limits can be taken simultaneously via $m\to\infty$. Since the voltage and current variables are conjugated $\vec{\lambda}$ is affected by the discretization as well:

$$\vec{\lambda}=\Delta\lambda\,\vec{l},\quad \Delta\lambda\Delta\theta=\pi/M, \tag{2.34}$$

where $\vec{l}$ is a $(D\times E)$-dimensional integer taking the same values as $\vec{k}$. This choice guarantees that the completeness and orthogonality relations

$$\frac{1}{(2M)^{DE}}\sum_{\vec{\theta}}\exp(i\vec{\lambda}\cdot\vec{\theta})=\delta_{\vec{\lambda},\vec{0}\ \mathrm{mod}(2M\Delta\lambda)} \tag{2.35a}$$

and

$$\frac{1}{(2M)^{DE}}\sum_{\vec{\lambda}}\exp(i\vec{\lambda}\cdot\vec{\theta})=\delta_{\vec{\theta},\vec{0}\ \mathrm{mod}(2M\Delta\theta)} \tag{2.35b}$$

do hold. Equation (2.35) provides us with a Fourier transform in replica space. In this discrete picture there are $(2M)^{DE}-1$ independent state variables per lattice site. Upon Fourier transformation one introduces the Potts spins [24]

$$\Phi_{\vec{\theta}}(x)=(2M)^{-DE}\sum_{\vec{\lambda}\neq\vec{0}}\exp(i\vec{\lambda}\cdot\vec{\theta})\psi_{\vec{\lambda}}(x)=\delta_{\vec{\theta},\vec{\theta}_x}-(2M)^{-DE} \tag{2.36}$$

subject to the condition $\Sigma_{\vec{\theta}}\Phi_{\vec{\theta}}(x)=0$.

Now we revisit Eq. (2.27). Carrying out the average over the diluted lattice configurations and the noise provides us with the weight $\exp(-H_{\mathrm{rep}})$ of the average $\langle\cdots\rangle_{\mathrm{rep}}$,

$$\begin{aligned}H_{\mathrm{rep}}&=-\ln\left\langle\left\{\exp\left[-\frac{1}{2}P(\{\vec{\theta}\})+\frac{i\omega}{2}\sum_i\vec{\theta}_i^{\,2}\right]\right\}_f\right\rangle_C\\&=-\sum_{\langle i,j\rangle}\ln\left\langle\prod_{\beta=1}^{E}\left\{\exp\left[-\frac{1}{2}\sigma_{i,j}^{(\beta)}(\vec{\theta}_i^{(\beta)}-\vec{\theta}_j^{(\beta)})^2\right]\right\}_f\right\rangle_C\\&\quad-\frac{i\omega}{2}\sum_i\vec{\theta}_i^{\,2}.\end{aligned} \tag{2.37}$$

By dropping a constant term $N_B\ln(1-p)$, with N_B being the number of bonds in the undiluted lattice, one obtains

$$\begin{aligned}H_{\mathrm{rep}}&=-\sum_{\langle i,j\rangle}K(\vec{\theta}_i-\vec{\theta}_j)-\sum_i h(\vec{\theta}_i)=-\sum_{\langle i,j\rangle}\sum_{\vec{\theta},\vec{\theta}'}K(\vec{\theta}\\&\quad-\vec{\theta}')\Phi_{\vec{\theta}}(i)\Phi_{\vec{\theta}'}(j)-\sum_i\sum_{\vec{\theta}}h(\vec{\theta})\Phi_{\vec{\theta}}(i),\end{aligned} \tag{2.38}$$

where

$$h(\vec{\theta})=\frac{i\omega}{2}\sum_i\vec{\theta}_i^{\,2} \tag{2.39}$$

and

$$\begin{aligned}K(\vec{\theta})&=\ln\left\{1+\frac{p}{1-p}\prod_{\beta=1}^{E}\left\{\exp\left[-\frac{1}{2}\sigma^{(\beta)}\sum_{\alpha=1}^{D}(\theta^{(\alpha,\beta)})^2\right]\right\}_f\right\}\\&=\ln\left\{1+\frac{p}{1-p}\exp\left[\sum_{l=1}^{\infty}\frac{(-1/2)^l}{l!}\Delta^{(l)}K_l(\vec{\theta})\right]\right\}.\end{aligned} \tag{2.40}$$

In the limit of perfect transport, $s\to 0$, $K(\vec{\theta})$ goes to its local limit $K(\vec{\theta})=K\delta_{\vec{\theta},\vec{0}}$, with K being a positive constant. The interaction part of the Hamiltonian reduces to

$$H_{\mathrm{rep}}^{\mathrm{int}}=-K\sum_{\langle i,j\rangle}\sum_{\vec{\theta}}\Phi_{\vec{\theta}}(i)\Phi_{\vec{\theta}}(j). \tag{2.41}$$

This represents nothing more than the $(2M)^{DE}$-state Potts model which is invariant against all $(2M)^{DE}!$ permutations of the Potts spins $\Phi_{\vec{\theta}}$.

In the case of imperfect transport this $S_{(2M)^{DE}}$ symmetry is lost. For finite $\overline{\sigma}$ and $\Delta^{(n)}=0$, $K(\vec{\theta})$ is an exponentially decreasing function in replica space with a decay rate proportional to $\overline{\sigma}^{-1}$. Then, for large $\overline{\sigma}$, the Hamiltonian H_{rep} describes a translationally and rotationally invariant short range interaction of Potts spins in real and replica space with an external one-site potential $h(\vec{\theta})$.

Admitting fluctuations of the resistances, $\Delta^{(n)}>0$, results in breaking the rotational $O(DE)$ replica space symmetry of the interaction part of the Hamiltonian. The Fourier transform of $K(\vec{\theta})$,

$$\tilde{K}(\vec{\lambda})=\frac{1}{(2M)^{DE}}\sum_{\vec{\theta}}\exp(-i\vec{\lambda}\cdot\vec{\theta})K(\vec{\theta}), \tag{2.42}$$

is expediently evaluated by switching back to continuous voltages,

$$\begin{aligned}\tilde{K}(\vec{\lambda})&=\int_{-\infty}^{\infty}d\vec{\theta}\exp(-i\vec{\lambda}\cdot\vec{\theta})\ln\left\{1+\frac{p}{1-p}\right.\\&\quad\left.\times\exp\left[\sum_{l=1}^{\infty}\frac{(-1/2)^l}{l!}\Delta^{(l)}K_l(\vec{\theta})\right]\right\},\end{aligned} \tag{2.43}$$

where we have dropped a factor $(2\theta_M)^{-DE}$. Taylor expansion of the logarithm yields a series of terms of the form

$$\int_{-\infty}^{\infty}d\vec{\theta}\exp\left[-i\vec{\lambda}\cdot\vec{\theta}-a\overline{\sigma}\vec{\theta}^2-\sum_{l=2}b_l(\overline{\sigma}s)^l K_l(\vec{\theta})\right], \tag{2.44}$$

where a the b_l are constants of order $O(s^0)$. In addition to the expansion of the logarithm we expand in a power series in s, so that Eq. (2.44) becomes

$$\int_{-\infty}^{\infty} d\vec{\theta}\exp[-i\vec{\lambda}\cdot\vec{\theta}-a\bar{\sigma}\vec{\theta}^2]\left\{1+\sum_{l=2}^{\infty}(\bar{\sigma}s)^l P_l(\vec{\theta})\right\}. \quad (2.45)$$

Here the P_l are homogeneous polynomials of order $2l$ in $\vec{\lambda}$ that are sums of terms proportional to

$$\prod_{i\geqslant 2} K_i(\vec{\theta})^{l_i} \quad (2.46)$$

such that $\Sigma_i i l_i = l$. Completing squares in the exponential in Eq. (2.45) gives

$$\begin{aligned}
&\exp\left[-\frac{\vec{\lambda}^2}{4a\bar{\sigma}}\right]\int_{-\infty}^{\infty} d\vec{\theta}\exp[-a\bar{\sigma}\vec{\theta}^2]\\
&\quad\times\left\{1+\sum_{l=2}^{\infty}(\bar{\sigma}s)^l P_l\left(\vec{\theta}-i\frac{\vec{\lambda}}{2a\bar{\sigma}}\right)\right\}\\
&=\exp\left[-\frac{\vec{\lambda}^2}{4a\bar{\sigma}}\right]\left\{1+\sum_{l=2}^{\infty}(\bar{\sigma}s)^l\right.\\
&\quad\left.\times\left[P_l\left(\frac{\vec{\lambda}}{\bar{\sigma}}\right)+\cdots+\bar{\sigma}^{(-r)}P_{l-r}\left(\frac{\vec{\lambda}}{\bar{\sigma}}\right)+\cdots\right]\right\}, \quad (2.47)
\end{aligned}$$

where we have omitted multiplicative factors decorating the P_l. Due to the homogeneity of the P_l, Eq. (2.47) can be rearranged as

$$\begin{aligned}
&\exp\left[-\frac{\vec{\lambda}^2}{4a\bar{\sigma}}\right]\left\{1+\sum_{l=2}^{\infty}s^l[\bar{\sigma}^{-l}P_l(\vec{\lambda})+\cdots\right.\\
&\quad\left.+\bar{\sigma}^{-(l-r)}P_{l-r}(\vec{\lambda})+\cdots]\right\}\\
&=\exp\left[-\frac{\vec{\lambda}^2}{4a\bar{\sigma}}\right]\left\{1+\sum_{l'=1}^{\infty}\left(\frac{s}{\bar{\sigma}}\right)^{l'}[1+O(s)]P_{l'}(\vec{\lambda})\right\}, \quad (2.48)
\end{aligned}$$

up to multiplicative factors. By keeping only the leading contributions, one finds that $\tilde{K}(\vec{\lambda})$ can be expanded as

$$\tilde{K}(\vec{\lambda})=\tau+\sum_{p=1}^{\infty}w_p\vec{\lambda}^{2p}+\sum_{P_l}v_{P_l}P_l(\vec{\lambda}), \quad (2.49)$$

with τ, $w_p\sim\bar{\sigma}^{-p}$, and $v_{P_l}\sim\Delta^{(l)}/\bar{\sigma}^{2l}$ being expansion coefficients.

It is known that the terms $w_p\vec{\lambda}^{2p}$ are irrelevant in the renormalization group sense for $p\geqslant 2$ (see, e.g., [20]). From Sec. II F it can be inferred that the $v_{P_l}P_l(\vec{\lambda})$ are irrelevant as well. However, the terms proportional to $K_l(\vec{\lambda})$ are indispensable in studying the noise cumulants; they are dangerously irrelevant. Therefore, we restrict the expansion of $\tilde{K}(\vec{\lambda})$ to

$$\tilde{K}(\vec{\lambda})=\tau+w\vec{\lambda}^2+\sum_{l=2}^{\infty}v_l K_l(\vec{\lambda}), \quad (2.50)$$

with $w=w_1$ and $v_l=v_{K_l}$. Nevertheless, the neglected terms will regain some importance later on since they are required for the renormalization of the v_l.

The K_l are homogeneous polynomials of order $2l$. For $l\geqslant 2$ they possess $S[O(D)^E]$ symmetry. Thus, allowing for $\Delta^{(n)}>0$ results in losing the rotational $O(DE)$ in favor of the $S[O(D)^E]$ symmetry.

It is worth pointing out that $v_l/w^l\sim\Delta^{(l)}/\bar{\sigma}^l\sim s^l$, i.e., the condition $s\to 0$ translates into $v_l\ll w^l$. Consequently one has to take the limit $v_l\to 0$ before the limit $w\to 0$ in calculating the exponents associated with the v_l.

We proceed with the usual coarse graining step and replace the Potts spins $\Phi_{\vec{\theta}}(x)$ by order parameter fields $\varphi(\mathbf{x},\vec{\theta})$ which inherit the constraint $\Sigma_{\vec{\theta}}\varphi(\mathbf{x},\vec{\theta})=0$. We model the corresponding field theoretic Hamiltonian $\mathcal{H}$ in the spirit of Landau as a mesoscopic free energy from local monomials of the order parameter field and its gradients in real and replica space. The gradient expansion is justified since the interaction is short ranged in both spaces. Purely local terms in replica space have to respect the full $S_{(2M)^{DE}}$ Potts symmetry. After these remarks we write down the Landau-Ginzburg-Wilson type Hamiltonian

$$\begin{aligned}
\mathcal{H}=\int d^dx\sum_{\vec{\theta}}&\left\{\frac{1}{2}\varphi(\mathbf{x},\vec{\theta})K(\Delta,\nabla_{\vec{\theta}})\varphi(\mathbf{x},\vec{\theta})\right.\\
&\left.+\frac{g}{6}\varphi(\mathbf{x},\vec{\theta})^3+\frac{i\omega}{2}\vec{\theta}^2\varphi(\mathbf{x},\vec{\theta})\right\}, \quad (2.51)
\end{aligned}$$

where

$$\begin{aligned}
K(\Delta,\nabla_{\vec{\theta}})=\tau+\Delta+w\sum_{\alpha,\beta=1}^{D,E}&\frac{-\partial^2}{(\partial\theta^{(\alpha,\beta)})^2}\\
&+\sum_{l=2}^{\infty}v_l\sum_{\beta=1}^{E}\left[\sum_{\alpha=1}^{D}\frac{-\partial^2}{(\partial\theta^{(\alpha,\beta)})^2}\right]^l. \quad (2.52)
\end{aligned}$$

In Eq. (2.51) we have neglected terms of order φ^4 or higher, which are irrelevant in the renormalization group sense. τ, w, and v_l are now coarse grained analogs of the original coefficients appearing in Eq. (2.50). Note again that $\mathcal{H}$ reduces to the usual $(2M)^{DE}$-state Potts model Hamiltonian by setting $v_l=0$ and $w=0$, as one retrieves purely geometrical percolation in the limit of vanishing v_l and w.

F. Relevance of the noise terms

Irrelevant variables that cannot be taken to zero because the quantity one is looking at either vanishes or diverges in this limit have been given the name *dangerously irrelevant variables* by Fisher [25]. Later on this notion was introduced into field theory by Amit and Peliti [26]. A characteristic feature of dangerously irrelevant variables is that corrections due to them determine the asymptotic behavior of quantities

with the above property, so that their effect is felt arbitrarily close to the transition [27]. In this section we show that the v_l are dangerously irrelevant. They are irrelevant on dimensional grounds, i.e., they are associated with a negative naive dimension. However, we cannot simply take the v_l to zero by appealing to their irrelevance, because the amplitudes of the noise cumulants vanish in this limit.

In the remainder of this article we focus on vanishing frequency $\omega=0$. Let $\mathcal{P}$ denote the set of parameters $\{\tau,w,v_l\}$. We introduce a scaling factor b for the voltage variable: $\vec{\theta}\to b\vec{\theta}$. By substitution of $\varphi(\mathbf{x},\vec{\theta})=\varphi'(\mathbf{x},b\vec{\theta})$ the Hamiltonian turns into

$$\mathcal{H}[\varphi'(\mathbf{x},b\vec{\theta}),\mathcal{P}]=\int d^dx\sum_{\vec{\theta}}\left\{\frac{1}{2}\varphi'(\mathbf{x},b\vec{\theta})K(\Delta,\nabla_{\vec{\theta}})\times\varphi'(\mathbf{x},b\vec{\theta})+\frac{g}{6}\varphi'(\mathbf{x},b\vec{\theta})^3\right\}. \quad (2.53)$$

Renaming the scaled voltage variables $\vec{\theta}'=b\vec{\theta}$ yields

$$\mathcal{H}[\varphi'(\mathbf{x},\vec{\theta}'),\mathcal{P}]=\int d^dx\sum_{\vec{\theta}'}\left\{\frac{1}{2}\varphi'(\mathbf{x},\vec{\theta}')K(\Delta,b\nabla_{\vec{\theta}'})\times\varphi'(\mathbf{x},\vec{\theta}')+\frac{g}{6}\varphi'(\mathbf{x},\vec{\theta}')^3\right\}. \quad (2.54)$$

Obviously the voltage cutoff is affected by the scaling as well: $\theta_M\to b\theta_M$. However, if the limits are taken in the appropriate order, namely, $D\to 0$ and then $m\to\infty$, the dependence of the theory on the cutoff drops out. Thus, we can identify $\vec{\theta}'$ and $\vec{\theta}$ and hence

$$\mathcal{H}[\varphi(\mathbf{x},b\vec{\theta}),\mathcal{P}]=\mathcal{H}[\varphi(\mathbf{x},\vec{\theta}),\mathcal{P}'], \quad (2.55)$$

where $\mathcal{P}'=\{\tau,b^2w,b^{2l}v_l\}$.

Now consider correlation functions

$$G_N(\{\mathbf{x},\vec{\theta}\};\tau,w,\{v_l\})=\int\mathcal{D}\varphi\,\varphi(\mathbf{x}_1,\vec{\theta}_1)\cdots\varphi(\mathbf{x}_N,\vec{\theta}_N)\times\exp\{-\mathcal{H}[\varphi(\mathbf{x},\vec{\theta}),\mathcal{P}]\}, \quad (2.56)$$

where $\mathcal{D}\varphi$ indicates an integration over the set of variables $\{\varphi(\mathbf{x},\vec{\theta})\}$ for all $\mathbf{x}$ and $\vec{\theta}$. Equation (2.55) implies

$$G_N(\{\mathbf{x},\vec{\theta}\};\tau,w,\{v_l\})=G_N(\{\mathbf{x},b\vec{\theta}\};\tau,b^2w,\{b^{2l}v_l\}). \quad (2.57)$$

The two-point correlation function G_2 is the Fourier transform of $\langle\psi_{\vec{\lambda}}(\mathbf{x})\psi_{-\vec{\lambda}}(\mathbf{x})\rangle_{\mathcal{H}}$. We deduce from Eq. (2.31) that

$$K_l(\vec{\lambda})C_R^{(l)}((\mathbf{x},\mathbf{x}');\tau,w,\{v_k\})=b^{-2l}K_l(\vec{\lambda})C_R^{(l)}((\mathbf{x},\mathbf{x}');\tau,b^2w,\{b^{2k}v_k\}). \quad (2.58)$$

We are free to choose $b^2=w^{-1}$. This gives

$$C_R^{(l)}((\mathbf{x},\mathbf{x}');\tau,w,\{v_k\})=w^l f_l\left((\mathbf{x},\mathbf{x}');\tau,\left\{\frac{v_k}{w^k}\right\}\right), \quad (2.59)$$

where f_l is a scaling function. We learn from Eq. (2.59) that the coupling constants v_k appear only as v_k/w^k. Dimensional analysis of the Hamiltonian shows that $w\vec{\lambda}^2\sim\mu^2$ and $v_kK_k(\vec{\lambda})\sim\mu^2$, where μ is an inverse length scale, i.e., $w\vec{\lambda}^2$ and $v_kK_k(\vec{\lambda})$ have a naive dimension 2. Thus $v_k/w^k\sim\mu^{2-2k}$ and hence the v_k/w^k have a negative naive dimension. This leads to the conclusion that the v_k are irrelevant couplings.

Though irrelevant, one must not set $v_l=0$ in calculating the noise exponents. In order to see this we expand the scaling function f_l in Eq. (2.59),

$$C_R^{(l)}((\mathbf{x},\mathbf{x}');\tau,w,\{v_k\})=w^l\left\{C_l^{(l)}\frac{v_l}{w^l}+C_{l+1}^{(l)}\frac{v_{l+1}}{w^{l+1}}+\cdots\right\}, \quad (2.60)$$

with $C_k^{(l)}$ being expansion coefficients depending on $\mathbf{x}$, $\mathbf{x}'$, and τ. It is important to recognize that $C_{k<l}^{(l)}=0$ because the corresponding terms are not generated in the perturbation calculation. Equation (2.60) can be rewritten as

$$C_R^{(l)}((\mathbf{x},\mathbf{x}');\tau,w,\{v_k\})=v_l\left\{C_l^{(l)}+C_{l+1}^{(l)}\frac{v_{l+1}}{wv_l}+\cdots\right\}, \quad (2.61)$$

where the first term on the right hand side gives the leading behavior. Thus $C_R^{(l)}$ vanishes upon setting $v_l=0$ and we cannot gain any further information about $C_R^{(l)}$. In particular, we cannot determine the associated noise exponent. In other words, the v_l are dangerously irrelevant in investigating the critical properties of the $C_R^{(l\geqslant 2)}$.

III. RENORMALIZATION GROUP ANALYSES

A. Diagrammatic expansion

The diagrammatic elements contributing to our renormalization group improved perturbation calculation are the three-point vertex $-g$ and the propagator

$$\frac{1-\delta_{\vec{\lambda},\vec{0}}}{\mathbf{p}^2+\tau+w\vec{\lambda}^2+\sum_{l=2}^{\infty}v_lK_l(\vec{\lambda})}=\frac{1}{\mathbf{p}^2+\tau+w\vec{\lambda}^2+\sum_{l=2}^{\infty}v_lK_l(\vec{\lambda})}-\frac{\delta_{\vec{\lambda},\vec{0}}}{\mathbf{p}^2+\tau}. \quad (3.1)$$

Note that we have switched to a $(\mathbf{p},\vec{\lambda})$ representation by employing Fourier transformation in real and replica space. The notation in Eq. (3.1) is somewhat symbolic. To treat the irrelevant terms $v_lK_l(\vec{\lambda})$ properly, we have to expand the propagator in a power series in the v_l and discard all contributions of higher than linear order in the v_l. In other words, the irrelevant terms have to be treated as insertions.

Equation (3.1) shows that the principal propagator decomposes into a propagator carrying $\vec{\lambda}$'s (conducting) and one not carrying $\vec{\lambda}$'s (insulating). This allows for a schematic

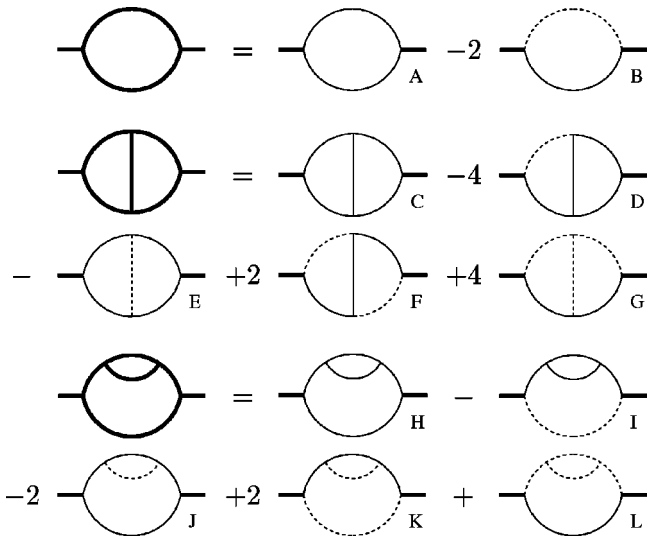

FIG. 1. Conducting diagrams to two-loop order. The bold lines symbolize principal propagators, the light lines stand for conducting, and the dashed lines for insulating propagators. We point out that the conducting diagrams inherit their combinatorial factor from their bold diagram. For example, the diagrams *A* and *B* have to be calculated with the same combinatorial factor 1/2.

decomposition of principal diagrams into sums of conducting diagrams consisting of conducting and insulating propagators. To two-loop order, we obtain the conducting diagrams listed in Fig. 1.

B. Multifractal moments of Feynman diagrams

From the decomposition in Sec. III A a real world interpretation of the conducting Feynman diagrams emerges [20,21]. They may be viewed as resistor networks themselves with conducting propagators corresponding to conductors and insulating propagators corresponding to open bonds. The parameters *s* appearing in a Schwinger parametrization of the conducting propagators,

$$\frac{1}{\mathbf{p}^2+\tau+w\vec{\vec{\lambda}}^2+\sum_{l=2}^{\infty} v_l K_l(\vec{\vec{\lambda}})} = \int_0^\infty ds\, \exp\left[-s\left(\mathbf{p}^2+\tau+w\vec{\vec{\lambda}}^2+\sum_{l=2}^{\infty} v_l K_l(\vec{\vec{\lambda}})\right)\right], \tag{3.2}$$

correspond to resistances and the replica variables $i\vec{\vec{\lambda}}$ to currents. The replica currents are conserved in each vertex and we may write for each edge i of a diagram $\vec{\vec{\lambda}}_i=\vec{\vec{\lambda}}_i(\vec{\vec{\lambda}},\{\vec{\vec{\kappa}}\})$, where $\vec{\vec{\lambda}}$ is an external current and $\{\vec{\vec{\kappa}}\}$ denotes a complete set of independent loop currents.

The real world interpretation suggests an effective way of computing the conducting diagrams. We learned from the discussion above that the irrelevant terms have to be treated by means of insertions,

$$\mathcal{O}^{(l)}=-\frac{1}{2}v_l\int d^dp\sum_{\vec{\vec{\lambda}}} K_l(\vec{\vec{\lambda}})\phi(\mathbf{p},\vec{\vec{\lambda}})\phi(-\mathbf{p},-\vec{\vec{\lambda}}), \tag{3.3}$$

where $\phi(\mathbf{p},\vec{\vec{\lambda}})$ denotes the Fourier transform of $\varphi(\mathbf{x},\vec{\vec{\theta}})$. The resulting diagrams are of the type displayed on the left hand side of Fig. 2. We express the current-dependent part of such a diagram in terms of its power *P*,

$$-s_i v_l\sum_{\{\vec{\vec{\kappa}}\}} K_l(\vec{\vec{\lambda}}_i)\exp\left[-w\sum_j s_j\vec{\vec{\lambda}}_j^2\right] = -s_i v_l\sum_{\{\vec{\vec{\kappa}}\}} K_l(\vec{\vec{\lambda}}_i)\exp[wP(\vec{\vec{\lambda}},\{\vec{\vec{\kappa}}\})]. \tag{3.4}$$

The summation is carried out by completing the squares in the exponential. The corresponding shift in the loop currents is given by the minimum of the quadratic form *P*, which is determined by a variation principle completely analogous to the one stated in Eq. (2.7). Thus, completing of the squares is equivalent to solving Kirchhoff's equations for the diagram. It leads to

$$-s_i v_l\sum_{\{\vec{\vec{\kappa}}\}} K_l\left(\vec{\vec{\lambda}}_i^{\,\mathrm{ind}}+\sum_j C_{i,j}(\{s\})\vec{\vec{\kappa}}_j\right) \times\exp\left[-wR(\{s\})\vec{\vec{\lambda}}^2-w\sum_{i,j} B_{i,j}(\{s\})\vec{\vec{\kappa}}_i\cdot\vec{\vec{\kappa}}_j\right]. \tag{3.5}$$

$\vec{\vec{\lambda}}_i^{\,\mathrm{ind}}=c_i(\{s\})\vec{\vec{\lambda}}$ is the current induced by the external current into edge *i*. $c_i(\{s\})$ and $C_{i,j}(\{s\})$ are homogeneous functions of the Schwinger parameters of degree zero. $B_{i,j}(\{s\})$ and the total resistance of the diagram $R(\{s\})$ are homogeneous functions of the Schwinger parameters of degree 1. By a suitable choice of the $\vec{\vec{\kappa}}_i$ the matrix constituted by the $B_{i,j}$ is rendered diagonal, i.e., $B_{i,j}\sim\delta_{i,j}$. At this stage it is convenient to switch to continuous currents and to replace the summation by an integration,

$$\sum_{\{\vec{\vec{\kappa}}\}}\rightarrow\int\prod_{i=1}^{L} d\vec{\vec{\kappa}}_i, \tag{3.6}$$

where $d\vec{\vec{\kappa}}$ is an abbreviation for $\Pi_{\alpha,\beta=1}^{D,E} d\kappa^{(\alpha,\beta)}$ and *L* stands for the number of independent conducting loops. This integration is Gaussian and therefore straightforward. In the limit $D\rightarrow 0$ one obtains

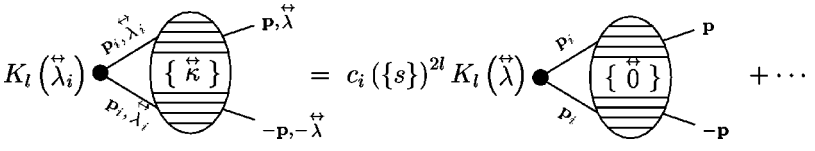

FIG. 2. Calculation scheme. The hatched ovals symbolize an arbitrary number of closed conducting loops. The solid dots indicate insertions.

$$-s_i v_l K_l(\overleftrightarrow{\lambda}_i^{\rm ind}) + \cdots = -s_i c_i(\{s\})^{2l} v_l K_l(\overleftrightarrow{\lambda}) + \cdots . \tag{3.7}$$

The terms neglected in Eq. (3.7) are not required in calculating the ψ_l. This issue is discussed in detail in Sec. III C. Diagrammatically, the calculation scheme can be condensed into Fig. 2. Appendix B illustrates the calculations in terms of an example.

So far we have inserted $\mathcal{O}^{(l)}$ only in one of the conducting propagators. However, each of them has to get an insertion. Moreover, the integrations over loop momenta and Schwinger parameters remain to be carried out. All in all, each diagram can be written as

$$\begin{aligned} I(\mathbf{p}^2,\overleftrightarrow{\lambda}) &= I_P(\mathbf{p}^2) - I_W(\mathbf{p}^2) w \overleftrightarrow{\lambda}^2 - I_V^{(l)}(\mathbf{p}^2) v_l K_l(\overleftrightarrow{\lambda}) + \cdots \\ &= \int_0^\infty \prod_i ds_i [1 - R(\{s_i\}) w \overleftrightarrow{\lambda}^2 - C^{(l)}(\{s_i\}) v_l K_l(\overleftrightarrow{\lambda}) \\ &\quad + \cdots] D(\mathbf{p}^2,\{s_i\}). \end{aligned} \tag{3.8}$$

Here $D(\mathbf{p}^2,\{s_i\})$ stands for the integrand one obtains upon Schwinger parametrization of the corresponding diagram in the usual ϕ^3 theory. $C^{(l)}(\{s_i\})$ is defined as

$$C^{(l)}(\{s_i\}) = \sum_i s_i c_i(\{s\})^{2l} = \sum_i s_i (\overleftrightarrow{\lambda}_i^{\rm ind}/\overleftrightarrow{\lambda})^{2l}, \tag{3.9}$$

where the sum runs over all conducting propagators of the diagram. Notice the analogy of the $C^{(l)}(\{s_i\})$ to the generalized multifractal moments we introduce in Appendix A. Thus, we refer to the $C^{(l)}(\{s_i\})$ as multifractal moments of conducting Feynman diagrams.

C. Renormalization and scaling

By employing dimensional regularization and minimal subtraction we proceed with standard techniques of renormalized field theory [28]. The renormalization of the v_l, however, involves some peculiarities that we will discuss in this section.

An operator $\mathcal{O}_i$ of a given naive dimension $[\mathcal{O}_i]$ inserted one time in a vertex function generates in general new primitive divergences corresponding to all operators of equal or lower naive dimension. Thus, one needs these newly generated operators as counterterms in the Hamiltonian.

The operators of lower naive dimension can be isolated by additive renormalization,

$$\mathcal{O}_i \to \hat{\mathcal{O}}_i = \mathcal{O}_i - \sum_{[\mathcal{O}_j]<[\mathcal{O}_i]} X_{i,j} \mathcal{O}_j . \tag{3.10}$$

Dimensional regularization in conjunction with minimal subtraction leads to $X_{i,j}$ containing at least a factor τ. These $X_{i,j}$ vanish at the critical point. Hence, the operators of lower naive dimension will not be considered in the following.

As argued in Sec. III B the term proportional to v_l in Eq. (3.8) is generated by inserting the operator $\mathcal{O}^{(l)}$. Inserting $\mathcal{O}^{(l)}$ into a diagram with n external legs (see Fig. 3) generates primitive divergences that must be canceled by counterterms of the structure

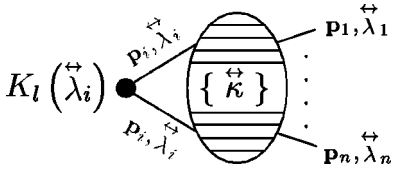

FIG. 3. $\mathcal{O}^{(l)}$ inserted into a diagram with n external legs.

$$P_r(\overleftrightarrow{\lambda}) \mathbf{p}^{2a} \phi(\mathbf{p},\overleftrightarrow{\lambda})^n, \tag{3.11}$$

where

$$P_r(\overleftrightarrow{\lambda}) = \prod_i K_i(\overleftrightarrow{\lambda})^{r_i} \tag{3.12}$$

with $\Sigma_i i r_i = r$ is a homogeneous polynomial of degree $2r$. Note that the notation we use here and in the following is symbolic, since such a counterterm has to depend on the entire set of external momenta and currents. $\phi(\mathbf{p},\overleftrightarrow{\lambda})^n$ is, for example, an abbreviation for $\Pi_{i=1}^n \phi(\mathbf{p}_i,\overleftrightarrow{\lambda}_i)$.

The leading contribution comes from operators having the same naive dimension as $\mathcal{O}^{(l)}$, i.e., those satisfying

$$2(l+2-3) = 2(r+a+n-3). \tag{3.13}$$

Here we expressed the naive dimension with the help of Eq. (C8). For $n=2$ one is led to $l \geqslant r$, i.e., the insertion of $\mathcal{O}^{(l)}$ generates operators containing homogeneous polynomials in the replica currents of degree equal to or lower than $2l$. In particular $\mathcal{O}^{(l)}$ generates an operator of type

$$v_l K_l(\overleftrightarrow{\lambda}) \phi(\mathbf{p},\overleftrightarrow{\lambda})^2. \tag{3.14}$$

The important question now is if the other operators generated by $\mathcal{O}^{(l)}$ generate operators of this type, too. Consider $n \geqslant 3$. With the help of Eq. (3.13) one obtains $l-1 \geqslant r \geqslant 1$, where the second inequality is a consequence of the limit $D \to 0$. Bearing in mind that maximal homogeneous polynomials of degree $l-1$ in $\overleftrightarrow{\lambda}$ are generated, we reinsert these operators of the type in Eq. (3.11) with $n \geqslant 3$ into two-leg diagrams (see Fig. 4). The resulting terms are of the form

$$P_{r'}(\overleftrightarrow{\lambda}) \mathbf{p}^{2a'} \phi(\mathbf{p},\overleftrightarrow{\lambda})^2, \tag{3.15}$$

with the leading contributions satisfying $r+a+n-3 = r'+a'-1$. Thus, $r' \geqslant r+a-a'+1$, i.e., the homogeneous polynomials in $\overleftrightarrow{\lambda}$ may have a higher degree than $2l$. However, they are of the type

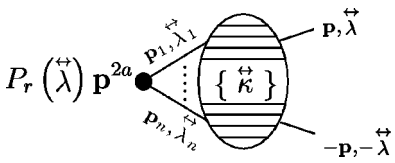

FIG. 4. An operator of the type in Eq. (3.11) with $n \geqslant 3$ inserted into a two-leg diagram.

$$P_{r'}(\overleftrightarrow{\lambda}) = K_1(\overleftrightarrow{\lambda})^s \prod_{2 \leqslant i \leqslant r} K_i(\overleftrightarrow{\lambda})^{r_i}, \tag{3.16}$$

with $\Sigma_i i r_i \leqslant r \leqslant l-1$ and $\Sigma_i i r_i + s = r'$. These polynomials have a higher symmetry than the original K_l.

We conclude that $\mathcal{O}^{(l)}$ generates itself and an entire family of new operators but these in turn do not generate $\mathcal{O}^{(l)}$. In principle, the entire family of operators associated with $\mathcal{O}^{(l)}$ has to be taken into account in the renormalization procedure, leading to a renormalization in matrix form,

$$\underline{\hat{\mathcal{O}}}^{(l)} \rightarrow \mathring{\underline{\hat{\mathcal{O}}}}^{(l)} = \underline{\underline{Z}}^{(l)} \underline{\hat{\mathcal{O}}}^{(l)}. \tag{3.17}$$

The vector

$$\underline{\hat{\mathcal{O}}}^{(l)} = (\mathcal{O}^{(l)}, \hat{\mathcal{O}}_2^{(l)}, \ldots) \tag{3.18}$$

contains the family associated with $\mathcal{O}^{(l)}$. For the remaining renormalizations, we employ the same scheme as in [20],

$$\varphi \rightarrow \mathring{\varphi} = Z^{1/2} \varphi, \quad \tau \rightarrow \mathring{\tau} = Z^{-1} Z_\tau \tau, \tag{3.19a}$$

$$w \rightarrow \mathring{w} = Z^{-1} Z_w w, \quad g \rightarrow \mathring{g} = Z^{-3/2} Z_u^{1/2} G_\epsilon^{-1/2} u^{1/2} \mu^{\epsilon/2}. \tag{3.19b}$$

In Eq. (3.19) ϵ stands for $6-d$ and the factor $G_\epsilon = (4\pi)^{-d/2} \Gamma(1+\epsilon/2)$, with Γ denoting the Gamma function, is introduced for convenience.

According to the arguments given above the renormalization matrix

$$\underline{\underline{Z}}^{(l)} = \underline{\underline{1}} + O(u) \tag{3.20}$$

has a particularly simple structure,

$$\underline{\underline{Z}}^{(l)} = \begin{pmatrix} Z^{(l)} & \diamondsuit & \cdots & \diamondsuit \\ 0 & \diamondsuit & \cdots & \diamondsuit \\ \vdots & \vdots & \ddots & \vdots \\ 0 & \diamondsuit & \cdots & \diamondsuit \end{pmatrix}, \tag{3.21}$$

where $\underline{\underline{1}}$ stands for the unit matrix and $\diamondsuit$ symbolizes elements that we do not evaluate. In this paper, we determine $Z^{(l)}$ to the order of two loops. Z, Z_τ, and Z_u are the usual Potts model Z factors. They have been computed to three-loop order by de Alcantara Bonfim *et al.* [29]. Z_w is known to two-loop order [20].

The unrenormalized theory has to be independent of the length scale μ^{-1} introduced by renormalization. In particular, the connected N-point correlation functions with an insertion of $\underline{\hat{\mathcal{O}}}^{(l)}$ must be independent of μ, i.e.,

$$\mu \frac{\partial}{\partial \mu} \mathring{G}_N(\{\mathbf{x}, \mathring{w}, \mathring{\overleftrightarrow{\lambda}}^2\}; \mathring{\tau}, \mathring{g})_{\underline{\hat{\mathcal{O}}}^{(l)}} = 0 \tag{3.22}$$

for all N. Equation (3.22) translates via the Wilson functions

$$\beta(u) = \mu \frac{\partial u}{\partial \mu}\bigg|_0, \quad \kappa(u) = \mu \frac{\partial \ln \tau}{\partial \mu}\bigg|_0, \tag{3.23a}$$

$$\zeta(u) = \mu \frac{\partial \ln w}{\partial \mu}\bigg|_0, \quad \gamma(u) = \mu \frac{\partial}{\partial \mu} \ln Z\bigg|_0, \tag{3.23b}$$

$$\underline{\underline{\gamma}}^{(l)}(u) = -\mu \frac{\partial}{\partial \mu} \ln \underline{\underline{Z}}^{(l)}\bigg|_0, \tag{3.23c}$$

where the bare quantities are kept fixed while taking the derivatives, into the Gell-Mann-Low renormalization group equation

$$\left\{ \left[\mu \frac{\partial}{\partial \mu} + \beta \frac{\partial}{\partial u} + \tau \kappa \frac{\partial}{\partial \tau} + w \zeta \frac{\partial}{\partial w} + \frac{N}{2} \gamma \right] \underline{\underline{1}} + \underline{\underline{\gamma}}^{(l)} \right\} \times G_N(\{\mathbf{x}, w \overleftrightarrow{\lambda}^2\}; \tau, u, \mu)_{\underline{\hat{\mathcal{O}}}^{(l)}} = 0. \tag{3.24}$$

The particular form of the Wilson functions can be extracted from the renormalization scheme and the Z factors. At the infrared stable fixed point u^*, determined by $\beta(u^*)=0$, the renormalization group equation reduces to

$$\left\{ \left[\mu \frac{\partial}{\partial \mu} + \tau \kappa^* \frac{\partial}{\partial \tau} + w \zeta^* \frac{\partial}{\partial w} + \frac{N}{2} \gamma^* \right] \underline{\underline{1}} + \underline{\underline{\gamma}}^{(l)*} \right\} \times G_N(\{\mathbf{x}, w \overleftrightarrow{\lambda}^2\}; \tau, u^*, \mu)_{\underline{\hat{\mathcal{O}}}^{(l)}} = 0, \tag{3.25}$$

where $\gamma^* = \gamma(u^*)$, $\kappa^* = \kappa(u^*)$, $\zeta^* = \zeta(u^*)$, and $\underline{\underline{\gamma}}^{(l)*} = \underline{\underline{\gamma}}^{(l)}(u^*)$.

The matrix $\underline{\underline{\gamma}}^{(l)}$ inherits the simple structure of $\underline{\underline{Z}}^{(l)}$,

$$\underline{\underline{\gamma}}^{(l)} = \begin{pmatrix} \gamma^{(l)} & \diamondsuit & \cdots & \diamondsuit \\ 0 & \diamondsuit & \cdots & \diamondsuit \\ \vdots & \vdots & \ddots & \vdots \\ 0 & \diamondsuit & \cdots & \diamondsuit \end{pmatrix}. \tag{3.26}$$

Owing to this structure, $|1\rangle = (1,0,\ldots,0)^T$ is a right eigenvector of $\underline{\underline{\gamma}}^{(l)*}$ with eigenvalue $\gamma^{(l)*}$. The remaining right eigenvectors with eigenvalues $\gamma_k^{(l)*}$, $k \geqslant 2$, we denote by $|k\rangle$. The left eigenvectors of $\underline{\underline{\gamma}}^{(l)*}$ are $\langle 1| = (1, \diamondsuit, \ldots, \diamondsuit)$ and $\langle k| = (0, \diamondsuit, \ldots, \diamondsuit)$. In terms of the eigenvectors, $\underline{\underline{\gamma}}^{(l)*}$ can be spectrally decomposed into

$$\underline{\underline{\gamma}}^{(l)*} = |1\rangle \gamma^{(l)*} \langle 1| + \sum_{k \geqslant 2} |k\rangle \gamma_k^{(l)*} \langle k|. \tag{3.27}$$

Now it is important to realize that

$$\langle 1| \underline{\hat{\mathcal{O}}}^{(l)} = \hat{\mathcal{O}}^{(l)} + \sum_{k \geqslant 2} \diamondsuit \hat{\mathcal{O}}_k^{(l)} = \mathcal{A}^{(l)},$$

$$\langle k| \underline{\hat{\mathcal{O}}}^{(l)} = \sum_{k \geqslant 2} \diamondsuit \hat{\mathcal{O}}_k^{(l)}, \tag{3.28}$$

i.e., only $\mathcal{A}^{(l)}$ contains the operator $\mathcal{O}^{(l)}$ we are interested in. We substitute Eq. (3.27) into the renormalization group equation (3.25) and act on the entire equation with $\langle 1|$. The result is

$$\left[\mu\frac{\partial}{\partial\mu}+\tau\kappa^*\frac{\partial}{\partial\tau}+w\zeta^*\frac{\partial}{\partial w}+\frac{N}{2}\gamma+\gamma^{(l)}\right]G_N(\{\mathbf{x},w\overleftrightarrow{\lambda}^2\};\tau,u^*,\mu)_{\mathcal{A}^{(l)}}=0. \quad (3.29)$$

Equation (3.29) is solved by the method of characteristics. The solution reads

$$G_N(\{\mathbf{x},w\overleftrightarrow{\lambda}^2\};\tau,u^*,\mu)_{\mathcal{A}^{(l)}} = \varrho^{\gamma^* N/2+\gamma^{(l)*}} \times G_N(\{\varrho\mathbf{x},\varrho^{\zeta^*}w\overleftrightarrow{\lambda}^2\};\ \varrho^{\kappa^*}\tau,u^*,\varrho\mu)_{\mathcal{A}^{(l)}}. \quad (3.30)$$

To derive a scaling relation for the correlation functions, a dimensional analysis remains to be performed. It yields

$$G_N(\{\mathbf{x},w\overleftrightarrow{\lambda}^2\};\tau,u,\mu)_{\mathcal{A}^{(l)}} = \mu^{(d-2)N/2-2} \times G_N(\{\mu\mathbf{x},\mu^{-2}w\overleftrightarrow{\lambda}^2\};\ \mu^{-2}\tau,u,1)_{\mathcal{A}^{(l)}}. \quad (3.31)$$

From Eqs. (3.30) and (3.31) we deduce the scaling behavior

$$G_N(\{\mathbf{x},w\overleftrightarrow{\lambda}^2\};\tau,u,\mu)_{\mathcal{A}^{(l)}} = \varrho^{(d-2+\eta)N/2-\psi_l/\nu} \times G_N(\{\varrho\mathbf{x},\varrho^{-\phi/\nu}w\overleftrightarrow{\lambda}^2\};\ \varrho^{-1/\nu}\tau,u^*,\mu)_{\mathcal{A}^{(l)}}. \quad (3.32)$$

$\eta=\gamma^*$ and $\nu=(2-\kappa^*)^{-1}$ are the well known critical exponents for percolation. They are known to third order in ϵ [29]:

$$\eta=\gamma^*=-\frac{1}{21}\epsilon-\frac{206}{9261}\epsilon^2+\left[-\frac{93\,619}{8\,168\,202}+\frac{256}{7203}\zeta(3)\right]\epsilon^3+O(\epsilon^4), \quad (3.33)$$

and

$$\nu=(2-\kappa^*)^{-1}=\frac{1}{2}+\frac{5}{84}\epsilon+\frac{589}{37\,044}\epsilon^2+\left[\frac{716\,519}{130\,691\,232}-\frac{89}{7203}\zeta(3)\right]\epsilon^3+O(\epsilon^4). \quad (3.34)$$

Note that ζ in Eqs. (3.33) and (3.34) stands for the Riemann zeta function and should not be confused with the Wilson function defined above. $\phi=\nu(2-\zeta^*)$ is the resistance exponent known to second order in ϵ [30,20],

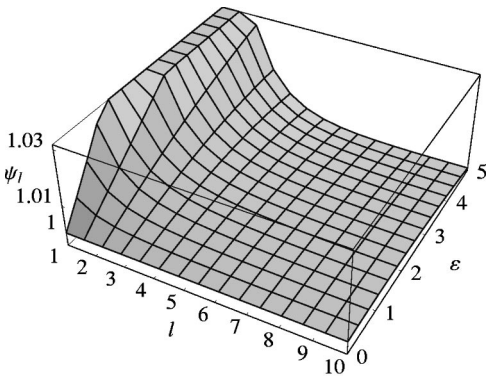

FIG. 5. Dependence of the noise exponents ψ_l on $\epsilon=6-d$.

$$\phi=\nu(2-\zeta^*)=1+\frac{1}{42}\epsilon+\frac{4}{3087}\epsilon^2+O(\epsilon^3). \quad (3.35)$$

The noise exponents ψ_l are defined by $\psi_l=\nu(2-\gamma^{(l)*})$. The expansion of ψ_l to second order in ϵ is given below.

Now we are in the position to derive the scaling behavior of $C_R^{(l)}$. From Eq. (3.32) we find upon choosing $\varrho=|\mathbf{x}-\mathbf{x}'|^{-1}$ and Taylor expanding that the two-point correlation function $G=G_2$ scales at criticality as

$$G(\mathbf{x},\mathbf{x}';\overleftrightarrow{\lambda})=|\mathbf{x}-\mathbf{x}'|^{2-d-\eta}\{1+w\overleftrightarrow{\lambda}^2|\mathbf{x}-\mathbf{x}'|^{\phi/\nu}+v_l K_l(\overleftrightarrow{\lambda})|\mathbf{x}-\mathbf{x}'|^{\psi_l/\nu}+\cdots\}, \quad (3.36)$$

where we have dropped several arguments for notational simplicity. With Eq. (2.33) the desired scaling behavior of $C_R^{(l)}$ is now readily obtained as

$$C_R^{(l)}\sim|\mathbf{x}-\mathbf{x}'|^{\psi_l/\nu}. \quad (3.37)$$

At this point, we emphasize once more the outstanding role of the $\mathcal{O}^{(l)}$, which warrants calling them master operators [23]. Each multifractal moment $M_l^{(l)}$ has a master operator as field theoretic counterpart. The master operators are highly and dangerously irrelevant in the renormalization group sense. Therefore, each master operator needs in general a myriad of other irrelevant operators for renormalization. However, the renormalization of these servant operators does not induce their master. It follows that the servant operators can be neglected in determining the scaling index of their master operator, i.e., one is spared the computation and diagonalization of giant renormalization matrices.

Our ϵ-expansion result for the noise exponents reads

$$\psi_l=1+\frac{\epsilon}{7(1+l)(1+2l)}+\frac{\epsilon^2}{12348(1+l)^3(1+2l)^3}\times[313-672\gamma+l(3327-4032\gamma-8l\{4(-389+273\gamma)+l[-2076+1008\gamma+l(-881+336\gamma)]\})-672(1+l)^2(1+2l)^2\Psi(1+2l)]+O(\epsilon^3), \quad (3.38)$$

in agreement to first order in ϵ with the one-loop calculation by PHL. $\gamma=0.577\,215\ldots$ denotes Euler's constant and Ψ

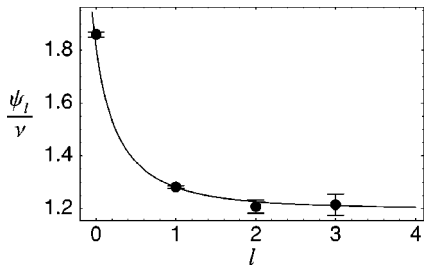

FIG. 6. Dependence of ψ_l/ν on l in three dimensions. The line shows our rationally approximated ϵ expansion. The numerical values, symbolized by the dots, are taken from Moukarzel [33] ($l=0$) and Batrouni *et al.* [18] ($l=1,2,3$). Moukarzel determined the backbone dimension $D_B=\psi_0/\nu$. Batrouni *et al.* studied the multifractal moments in a fixed voltage ensemble, i.e., for fixed externally applied voltage. The authors state a formula for switching from the multifractal exponents for the fixed voltage ensemble to those for the fixed current ensemble. In this formula a minus sign appears to be missing. Correctly, their exponents $x(n)$ are related to the ψ_l/ν via $\psi_l/\nu=2l\,x(2)-x(2l)$.

stands for the Digamma function [31]. Equation (3.38) is valid not only for $l\geqslant 2$ since it can be continued analytically down to $l=0$. A plot of ψ_l versus ϵ is given in Fig. 5. We point out that Eq. (3.38) evaluated at $l=1$ is in conformity with the result for ϕ stated in Eq. (3.35), i.e., our result for ψ_l satisfies an important consistency check stemming from $C_R^{(1)}=M_R^{(1)}$. Blumenfeld *et al.* [32] proved that ψ_l is a convex monotonically decreasing function of l. Note from Fig. 5 that our result for ψ_l captures this feature for reasonable values of ϵ. It reduces to unity in the limit $l\to\infty$ as one expects from the relation of ψ_∞ to the fractal dimension of the red bonds (see Appendix G). Moreover, analytic continuation of ψ_l to $l=0$ shows that $\psi_0=\nu D_B$ up to order $O(\epsilon^3)$ as expected (see Appendix G).

IV. COMPARISON TO NUMERICAL DATA

In this section we compare our result for ψ_l to numerical values. Instead of working with ψ_l directly we compare ψ_l/ν because data for exponents of this type are available in the literature. For the comparison it is not sufficient to simply evaluate Eq. (3.38) at $\epsilon=3$ or $\epsilon=4$. The pure ϵ expansion gives poor quantitative predictions for small spatial dimension. However, one can improve the ϵ expansion by incorporating rigorously known features. We carry out a rational approximation which takes into account that $\psi_l/\nu=1$ in one dimension. In practice this is done by adding an appropriate third-order term to the ϵ expansion of ψ_l/ν. We refrain from stating the formula so obtained explictly because it is a little lengthy. Instead we plot it for $\epsilon=3$, i.e., $d=3$, in Fig. 6. Our analytic result shows remarkable agreement with the available numerical data for $d=3$ [33,18]. For $l=0$ our result lies slightly outside the error bars of the simulations. However, the deviation of the values is less than 3%. For $l=1,2,3$ our result is within the error bars of the simulation. There are also numerical values available for $d=2$ [34,11]. Here, however, the agreement is much less pronounced. For $l=0,1,2,3,4$ we find a deviation of the order of 30%. It appears that the dependence of ψ_l on dimensionality is too rich in structure to be approximated well at $d=2$ by a series of a few terms.

V. CONCLUSIONS

We studied the multifractal moments of the current distribution in RRN's by renormalized field theory. Our approach thrived on two cornerstones. First, the Feyman diagrams for RRN's can be interpreted as being resistor networks themselves. In this paper we extended our real world interpretation by introducing multifractal moments for Feynman diagrams. The real world interpretation proves to be a powerful tool which allows a highly efficient calculation of the diagrams.

The second cornerstone was our concept of master operators. Whereas the field theoretic operator associated with the resistance exponent ϕ is relevant in the renormalization group sense, the operators associated with the $\psi_{l\geqslant 2}$ are dangerously irrelevant master operators. Due to their irrelevance the master operators generate a multitude of other irrelevant operators, the servants, which in principle must all be taken into account in the renormalization procedure. The servants, however, do not influence the scaling index of their master. Without this property, one would have to compute and diagonalize entire renormalization matrices for determining the ψ_l. These renormalization matrices are giants for large l. Without the master property it would be essentially impossible to compute the ψ_l for arbitrary l.

To our knowledge this is the first time that an entire family of multifractal exponents has been calculated to two-loop order, at least for percolation. Our result is for dimensions near the upper critical dimension 6 the most accurate analytic estimate for the ψ_l that we know of. It fulfils several consistency checks. Moreover, it agrees remarkably well with numerical data for $d=3$. As one expects, the agreement suffers on further decreasing the dimension. The dependence of the ψ_l on dimensionality appears to be too complex for good approximation at $d=2$ by a series of a few terms.

We expect that our concept of master operators can be applied to other systems showing multifractality. It works, for example, to describe the moments of the current distribution in random resistor diode networks. A two-loop calculation of the corresponding family of mutifractal exponents will be reported in the near future [35]. Another example for the applicability of the concept of master operators is the problem of diffusion near polymers. For this problem von Ferber and Holovatch [40] formulated a field theory that comprises dangerously irrelevant operators. Due to the symmetry properties of their operators no other irrelevant operators are generated in the perturbation calculations of these authors. Thus, the operators studied by von Ferber and Holovatch are particularly simple instances of master operators. Their scaling index is not influenced by any other operator simply because the number of their servants is zero. In this sense these master operators may be called poor.

It might turn out that the field theoretic operators associated with multifractal quantities are in general master operators. In this case the concept of master operators would be a

key in understanding the origin of multifractality, at least from a field theoretic point of view.

ACKNOWLEDGMENT

We acknowledge support by the Sonderforschungsbereich 237 ''Unordnung und große Fluktuationen'' of the Deutsche Forschungsgemeinschaft.

APPENDIX A: GENERALIZATION OF COHN'S THEOREM AND GENERALIZED MULTIFRACTAL MOMENTS

Consider a generalized power of the form

$$P(\{I_b\})=\sum_b \rho_b F(I_b), \tag{A1}$$

where F is some function of bond currents I_b. As argued in Sec. II, I_b is in general a function of the external current I and a complete set of loop currents $\{I^{(l)}\}$. We can exploit the variation principle (2.7) to eliminate the loop currents. As a result we obtain the I_b as a function of I and $\{\rho_b\}$ only. The solutions we denote by $I_b^{\rm ind}$. The derivative of the power $P(\{I_b^{\rm ind}\})$ so obtained with respect to bond resistance ρ_b reads

$$\frac{\partial P(\{I_b^{\rm ind}\})}{\partial \rho_b}=F(I_b^{\rm ind})+\sum_l \sum_{b'} \rho_{b'} \frac{\partial F(I_{b'}^{\rm ind})}{\partial I^{(l)}} \frac{\partial I^{(l)}}{\partial \rho_b}. \tag{A2}$$

The second term on the right hand side vanishes by virtue of the variation principle (2.7),

$$\frac{\partial P(\{I_b^{\rm ind}\})}{\partial I^{(l)}}=\sum_b \rho_b \frac{\partial F(I_{b'}^{\rm ind})}{\partial I^{(l)}}=0. \tag{A3}$$

Renaming $I_b=I_b^{\rm ind}$ we finally obtain

$$\frac{\partial P(\{I_b\})}{\partial \rho_b}=F(I_b) \tag{A4}$$

as a generalization of Cohn's theorem. For $F(I_b)=I_b^2$ one retrieves the original theorem

$$\frac{\partial R(x,x')}{\partial \rho_b}=\left(\frac{I_b}{I}\right)^2. \tag{A5}$$

Having generalized the power it is natural to generalize the multifractal moments as well. Consider the cumulants of the generalized power,

$$\{P^n\}_f^{(c)}=\frac{\partial^n}{\partial \lambda^n}\ln\{\exp(\lambda P)\}_f. \tag{A6}$$

In analogy to the resistance cumulants one finds for the leading behavior in the limit $s\to 0$

$$\{P^n\}_f^{(c)}=\sum_b \left(\left.\frac{\partial P}{\partial \rho_b}\right|_{\overline{\rho}}\right)^n \{\delta\rho_b^n\}_f^{(c)}=\sum_b F(I_b)^n \{\delta\rho_b^n\}_f^{(c)}. \tag{A7}$$

For networks like those described in Sec. II one has $\{\delta\rho_b^n\}_f^{(c)}=v_n$. However, in a more general situation the individual bonds may be composed of a series of elementary resistors. The elementary resistors are assumed to have independently and identically distributed resistances with mean $\overline{\rho}$ and higher cumulants $v_{l\geqslant 2}$. Then

$$\{\delta\rho_b^n\}_f^{(c)}=n_b v_n=\frac{\overline{\rho_b}}{\overline{\rho}} v_n, \tag{A8}$$

where n_b denotes the number of elementary resistors constituting bond b and $\overline{\rho_b}$ is the average resistance of that bond. Upon incorporating a factor $\overline{\rho}^{-1}$ into the constants v_n we finally find

$$\{P^n\}_f^{(c)}=v_n \sum_b \overline{\rho_b} F(I_b)^n, \tag{A9}$$

with $\Sigma_b \overline{\rho_b} F(I_b)^n$ being the nth multifractal moment of $F(I_b)$.

APPENDIX B: COMPUTATION OF DIAGRAMS: I

In this Appendix we illustrate the calculation scheme sketched in Sec. III B for diagram A (see Fig. 1). For the sake of simplicity, we focus on its contribution to the renormalization of v_2. We neglect all other parts and obtain

$$\mathrm{A}=-\int_0^\infty ds_1 ds_2 D(\mathbf{p}^2,\{s_i\}) \sum_{\overleftrightarrow{\kappa}} \exp[wP(\overleftrightarrow{\lambda},\overleftrightarrow{\kappa})] \times\{s_1 v_2 K_2(\overleftrightarrow{\kappa})+s_2 v_2 K_2(\overleftrightarrow{\kappa}+\overleftrightarrow{\lambda})\}, \tag{B1}$$

where $P(\overleftrightarrow{\lambda},\overleftrightarrow{\kappa})=-s_1\overleftrightarrow{\kappa}^2-s_2(\overleftrightarrow{\kappa}+\overleftrightarrow{\lambda})^2$ is, according to the real world interpretation, the power of the diagram, and $D(\mathbf{p}^2,\{s_i\})$ stands for

$$D(\mathbf{p}^2,\{s_i\})=\frac{g^2}{2}\int_{\mathbf{q}} \exp[-(s_1+s_2)\tau-s_1\mathbf{q}^2-s_2(\mathbf{q}+\mathbf{p})^2] \tag{B2}$$

with $\int_{\mathbf{q}}$ being an abbreviation for $(2\pi)^{-d/2}\int d^d q$. It is convenient to switch back to continuous currents and replace the summation over the loop current by an integration,

$$A=-\int_0^\infty ds_1 ds_2 D(\mathbf{p}^2,\{s_i\}) \int_{-\infty}^\infty d\overleftrightarrow{\kappa} \exp[wP(\overleftrightarrow{\lambda},\overleftrightarrow{\kappa})] \times\{s_1 v_2 K_2(\overleftrightarrow{\kappa})+s_2 v_2 K_2(\overleftrightarrow{\kappa}+\overleftrightarrow{\lambda})\}. \tag{B3}$$

The integration over the loop current is simplified by completing the squares in the exponential. One looks for the minimum of the quadratic form $P(\overleftrightarrow{\lambda},\overleftrightarrow{\kappa})$. The minimum is determined by a variation principle completely analogous to the one stated in Eq. (2.7). Thus completing the squares is equivalent to solving Kirchhoff's equations for the diagram. We obtain

$$A=-\int_0^\infty ds_1 ds_2 D(\mathbf{p}^2,\{s_i\})\exp[-R(\{s_i\})w\vec{\lambda}^2]$$
$$\times\int_{-\infty}^{\infty} d\vec{\kappa}\exp[-(s_1+s_2)w\vec{\kappa}^2]\Big\{s_1 v_2 K_2$$
$$\times\left(\vec{\kappa}-\frac{s_2}{s_1+s_2}\vec{\lambda}\right)+s_2 v_2 K_2\left(\vec{\kappa}+\frac{s_1}{s_1+s_2}\vec{\lambda}\right)\Big\}, \quad \text{(B4)}$$

where $R(\{s_i\})=s_1 s_2/(s_1+s_2)$ is the total resistance of the diagram. Note that $s_2\vec{\lambda}/(s_1+s_2)$ is, apart from a factor i, the replica current induced by the external replica current $\vec{\lambda}$ in the propagator parametrized by s_1. $s_1\vec{\lambda}/(s_1+s_2)$ is the replica current induced in the propagator parametrized by s_2. In the limit $D\to 0$ we find

$$A=-g^2\frac{1}{(4\pi)^{d/2}}\int_0^\infty\frac{ds_1 ds_2}{(s_1+s_2)^{d/2}}$$
$$\times\exp[-(s_1+s_2)\tau-R(\{s_i\})(\mathbf{p}^2+w\vec{\lambda}^2)]$$
$$\times\left\{\frac{s_1 s_2^4}{(s_1+s_2)^4}v_2 K_2(\vec{\lambda})+2\frac{s_1 s_2^2}{(s_1+s_2)^3}\frac{v_2}{w}\vec{\lambda}^2\right\}, \quad \text{(B5)}$$

where we have carried out the momentum integration as well. Expanding the exponential and keeping only the terms proportional to v_2 gives

$$A=-g^2\frac{1}{(4\pi)^{d/2}}\int_0^\infty\frac{ds_1 ds_2}{(s_1+s_2)^{d/2}}\exp[-(s_1+s_2)\tau]$$
$$\times\left\{\frac{s_1 s_2^4}{(s_1+s_2)^4}v_2 K_2(\vec{\lambda})+2\frac{s_1 s_2^2}{(s_1+s_2)^3}\frac{v_2}{w}\vec{\lambda}^2\right.$$
$$-2\frac{s_1^2 s_2^3}{(s_1+s_2)^4}\frac{v_2}{w}\vec{\lambda}^2(\mathbf{p}^2+w\vec{\lambda}^2)$$
$$\left.-\frac{s_1^2 s_2^5}{(s_1+s_2)^5}v_2 K_2(\vec{\lambda})(\mathbf{p}^2+w\vec{\lambda}^2)\right\}. \quad \text{(B6)}$$

The integral over the last term is convergent and therefore neglected. The remaining integrations are rendered straightforward by the change of variables $s_1\to tx$ and $s_2\to t(1-x)$. Upon expanding the result for small $\epsilon=6-d$ we obtain

$$A=-g^2\frac{G_\epsilon}{\epsilon}\tau^{-\epsilon/2}$$
$$\times\left\{\frac{1}{15}v_2 K_2(\vec{\lambda})-\frac{1}{3}\frac{v_2}{w}\vec{\lambda}^2\tau-\frac{1}{15}\frac{v_2}{w}\vec{\lambda}^2(\mathbf{p}^2+w\vec{\lambda}^2)\right\}, \quad \text{(B7)}$$

where we have introduced $G_\epsilon=(4\pi)^{(-d/2)}\Gamma(1+\epsilon/2)$ for convenience. We learn that not only primitive divergences proportional to $K_2(\vec{\lambda})$ but also those proportional to $\tau\vec{\lambda}^2$, $\mathbf{p}^2\vec{\lambda}^2$ and $(\vec{\lambda}^2)^2$ are generated.

APPENDIX C: SUPERFICIAL DEGREE OF DIVERGENCE OF OPERATOR INSERTIONS

Consider the insertion of a local operator $\mathcal{O}$ by adding a term to the Hamiltonian,

$$\mathcal{H}\to\mathcal{H}+\int d^d x\sum_{\vec{\theta}}\mathcal{O}(\mathbf{x},\vec{\theta}), \quad \text{(C1)}$$

where $\mathcal{O}$ is a local monomial of degree n in the fields φ with A derivatives in real and B derivatives in replica space. In a diagram composed of P propagators, V three-leg vertices, and the insertion there are

$$L=P-(V+1)-1 \quad \text{(C2)}$$

loops. The topological relation

$$3V+n=2P+E \quad \text{(C3)}$$

balances the number of legs. Each propagator behaves for large momenta as $1/\mathbf{q}^2$ and hence reduces the superficial degree of divergence of the diagram by 2. The insertion increases it by $A+B$. Thus the superficial degree of divergence $\delta[\mathcal{O}]$ of the diagram with insertion is

$$\delta[\mathcal{O}]=dL+A+B-2P. \quad \text{(C4)}$$

With help of Eqs. (C2) and (C3) one finds

$$\delta[\mathcal{O}]=\frac{d-6}{2}V+\frac{d-2}{2}n+\frac{2-d}{2}E+A+B. \quad \text{(C5)}$$

In contrast, the superficial degree of divergence δ of the diagram without insertion is

$$\delta=d+\frac{d-6}{2}V+\frac{2-d}{2}E. \quad \text{(C6)}$$

The difference

$$\delta[\mathcal{O}]-\delta=\frac{d-2}{2}n+A+B-d \quad \text{(C7)}$$

is identical to the naive dimension $[\mathcal{O}]$ of the insertion. For $d=6$ it reduces to

$$[\mathcal{O}]=2n+A+B-d. \quad \text{(C8)}$$

APPENDIX D: COMPUTATION OF DIAGRAMS: II

Here we give details of the calculation of the conducting Feynman diagrams listed in Fig. 1 for arbitrary l. We focus on the contributions of the diagrams to the renormalization of the v_l, i.e., those terms appearing in Eq. (3.8) proportional to v_l. The other terms appearing in Eq. (3.8) will be omitted throughout the entire Appendix for the sake of notational simplicity. For details of the calculation of the contributions to the renormalization of w we refer to [20]. The $\vec{\lambda}$-independent parts of the conducting diagrams correspond to the usual diagrams found in the literature on the Potts model [24] and can be calculated by standard proceedures [28].

We start with diagram A. The part of A required in the calculation of ψ_l reads for vanishing external momentum

$$A=-\frac{g^2}{2}v_l K_l(\overleftrightarrow{\lambda})\int_0^\infty ds_1 ds_2 \int_{\mathbf{q}} \exp[-(s_1+s_2)(\tau+\mathbf{q}^2)] \times\left\{ s_1\left(\frac{s_2}{s_1+s_2}\right)^n + s_2\left(\frac{s_1}{s_1+s_2}\right)^n\right\}, \tag{D1}$$

where $n=2l$. Carrying out the momentum integration gives

$$A=-g^2 v_l K_l(\overleftrightarrow{\lambda})\frac{1}{(4\pi)^{d/2}}\int_0^\infty ds_1 ds_2 \frac{1}{(s_1+s_2)^{d/2}} \times\exp[-(s_1+s_2)\tau]\frac{s_1 s_2^n}{(s_1+s_2)^n}. \tag{D2}$$

Changing variables, $s_1\to t(1-x)$ and $s_2\to tx$, leads to

$$A=-g^2 v_l K_l(\overleftrightarrow{\lambda})\frac{1}{(4\pi)^{d/2}}\int_0^1 dx(1-x)x^n \times\int_0^\infty dt t^{2-d/2}\exp(-t\tau) =-g^2 v_l K_l(\overleftrightarrow{\lambda})\frac{1}{(4\pi)^{d/2}}\frac{1}{(n+1)(n+2)}\Gamma\left(3-\frac{d}{2}\right)\tau^{d/2-3}. \tag{D3}$$

Expansion for small $\epsilon=6-d$ yields

$$\mathrm{A}=-g^2 v_l K_l(\overleftrightarrow{\lambda})\frac{2}{(n+1)(n+2)}\frac{G_\epsilon}{\epsilon}\tau^{-\epsilon/2}. \tag{D4}$$

The calculation of B is particularly simple. Thus we merely state the result

$$\mathrm{B}=-g^2 v_l K_l(\overleftrightarrow{\lambda})\frac{G_\epsilon}{2\epsilon}\tau^{-\epsilon/2}. \tag{D5}$$

Now we turn to the two-loop diagrams. As an example, we consider the diagram C. As a first step, we determine the currents flowing through the conducting propagators. Kirchhoff's law Eq. (2.5) applies to the four vertices of the diagram. This allows us to eliminate three of the five unknown currents (one of the vertices is inactive with respect to this purpose since the external current $\overleftrightarrow{\lambda}$ must be conserved). The potential drop around closed loops is zero. Hence we can eliminate the two remaining unknown currents and express all currents flowing through conducting propagators in terms of the Schwinger parameters and $\overleftrightarrow{\lambda}$. The momentum integrations are straightforward. They can be done by using the saddle point method, which works exactly here since the momentum dependence is purely quadratic. After the momentum integration we have

$$C=-\frac{g^4}{2}v_l K_l(\overleftrightarrow{\lambda})\frac{1}{(4\pi)^d}\int_0^\infty\prod_{i=1}^5 ds_i \frac{\exp\left(-\tau\sum_{i=1}^5 s_i\right)}{[(s_1+s_2+s_5)(s_3+s_4+s_5)-s_5^2]^{d/2}}\left\{ s_1\left[\frac{s_2(s_3+s_4+s_5)+s_4 s_5}{(s_1+s_2+s_5)(s_3+s_4+s_5)-s_5^2}\right]^n + s_2\left[\frac{s_1(s_3+s_4+s_5)+s_3 s_5}{(s_1+s_2+s_5)(s_3+s_4+s_5)-s_5^2}\right]^n + s_3\left[\frac{s_4(s_3+s_4+s_5)+s_2 s_5}{(s_1+s_2+s_5)(s_3+s_4+s_5)-s_5^2}\right]^n + s_4\left[\frac{s_3(s_3+s_4+s_5)+s_1 s_5}{(s_1+s_2+s_5)(s_3+s_4+s_5)-s_5^2}\right]^n + s_5\left[\frac{s_2 s_3-s_1 s_4}{(s_1+s_2+s_5)(s_3+s_4+s_5)-s_5^2}\right]^n\right\}$$

$$=-\frac{g^4}{2}v_l K_l(\overleftrightarrow{\lambda})\frac{1}{(4\pi)^d}\int_0^\infty\prod_{i=1}^5 ds_i \frac{\exp\left(-\tau\sum_{i=1}^5 s_i\right)}{[(s_1+s_2+s_5)(s_3+s_4+s_5)-s_5^2]^{d/2+n}} \times\{4s_1[s_2(s_3+s_4+s_5)+s_4 s_5]^n+s_5[s_2 s_3-s_1 s_4]^n\}. \tag{D6}$$

At this stage, the change of variables $s_1\to t_1(1-x)$, $s_2\to t_1 x$, $s_3\to t_2(1-y)$, $s_4\to t_2 y$, and $s_5\to t_3$ turns out to be useful. It leads to

$$C=-\frac{g^4}{2}v_l K_l(\overleftrightarrow{\lambda})\frac{1}{(4\pi)^d}\int_0^\infty dt_1 dt_2 dt_3\int_0^1 dx dy\frac{\exp[-\tau(t_1+t_2+t_3)]}{[t_1 t_2+t_2 t_3+t_1 t_3]^{d/2+n}}t_1 t_2 \times\{4t_1(1-x)[x t_1(t_2+t_3)+y t_2 t_3]^n+t_3(t_1 t_2)^n[x-y]^n\}. \tag{D7}$$

The integrations over x and y are straightforward and can be looked up in a table [36]. After some additional algebra we obtain

$$C=-\frac{g^4}{2}v_l K_l(\overleftrightarrow{\lambda})\frac{1}{(4\pi)^d}\int_0^\infty dt_1dt_2dt_3\frac{\exp[-\tau(t_1+t_2+t_3)]}{[t_1t_2+t_2t_3+t_1t_3]^{d/2}}$$
$$\times\left\{\frac{2}{(n+1)(n+2)}\frac{t_3(t_1t_2)^{n+1}}{[t_1t_2+t_2t_3+t_1t_3]^n}+\frac{4}{(n+1)(n+2)(n+3)}\frac{t_3[t_1t_2+t_2t_3+t_1t_3]^2}{t_1(t_1+t_2)}\right.$$
$$+\frac{4}{(n+1)(n+2)(n+3)}\frac{t_1[t_1t_2+t_2t_3+t_1t_3]^2}{(t_1+t_2)^2}-\frac{4}{(n+1)(n+2)(n+3)}\frac{t_3^{n+3}(t_1+t_2)^{n+1}}{t_1[t_1t_2+t_2t_3+t_1t_3]^n}$$
$$\left.-\frac{4}{(n+1)(n+2)(n+3)}\frac{t_1^{n+3}t_2^{n+2}}{(t_1+t_2)^2[t_1t_2+t_2t_3+t_1t_3]^n}-\frac{4}{(n+1)(n+2)}\frac{t_3t_1^{n+2}t_2^{n+1}}{(t_1+t_2)[t_1t_2+t_2t_3+t_1t_3]^n}\right\}. \quad \text{(D8)}$$

We find it convenient to express the remaining integrals in terms of the parameter integrals given in Appendix E. For the sake of notational simplicity we introduce the notation

$$M^\mu_{i,j,k}=(-1)^{i+j+k}\frac{\partial^{i+j+k}}{\partial a^i\partial b^j\partial c^k}M^\mu(a,b,c)|_{a=b=c=\tau}, \quad \text{(D9)}$$

where $\mu\in\{1,3,4\}$, and

$$M^\mu_{i,j,k}(n)=(-1)^{i+j+k}\frac{\partial^{i+j+k}}{\partial a^i\partial b^j\partial c^k}M^\mu(a,b,c;n)|_{a=b=c=\tau}, \quad \text{(D10)}$$

where $\mu\in\{5,6,7,8\}$. In terms of the parameter integrals we obtain

$$C=-\frac{g^4}{2}v_l K_l(\overleftrightarrow{\lambda})\left\{\frac{2}{(n+1)(n+2)}[M^8_{1,0,0}(n)\right.$$
$$-2M^7_{2,0,1}(n)-4M^7_{1,1,1}(n)-2M^7_{0,2,1}(n)]$$
$$+\frac{4}{(n+1)(n+2)(n+3)}[M+M^3_{2,0,0}+M^3_{1,1,0}$$
$$\left.-M^6_{1,0,0}(n)-M^6_{0,1,0}(n)-M^7_{3,0,0}(n)-M^7_{2,1,0}(n)]\right\}. \quad \text{(D11)}$$

The final result reads

$$\mathrm{C}=-\frac{g^4}{2}v_l K_l(\overleftrightarrow{\lambda})\frac{G_\epsilon^2}{\epsilon}\tau^{-\epsilon}\left\{\frac{4n+12}{(n+1)(n+2)(n+3)\epsilon}\right.$$
$$\left.+\frac{4n-2F_2(n+3)+12}{(n+1)(n+2)(n+3)}-\frac{2}{(n+1)(n+2)^2(n+3)}\right\}. \quad \text{(D12)}$$

The diagrams *D* to *G* can be evaluated in the same fashion.

As another example we consider diagram *H*. Determination of the noise cumulants of *H* leads to

$$H=-\frac{g^4}{2}v_l K_l(\overleftrightarrow{\lambda})\frac{1}{(4\pi)^d}$$
$$\times\int_0^\infty\prod_{i=1}^5 ds_i\frac{\exp\left(-\tau\sum_{i=1}^5 s_i\right)}{[(s_1+s_2+s_5)(s_3+s_4)+s_3s_4]^{d/2+n}}$$
$$\times\{2s_1[s_5(s_3+s_4)]^n+2s_3[s_4s_5]^n$$
$$+s_5[(s_1+s_2)(s_3+s_4)+s_3s_4]^n\}. \quad \text{(D13)}$$

Here, the change of variables $s_5\to t_1x$, $s_1\to t_1y$, $s_2\to t_1(1-x-y)$, $s_3\to t_2$, and $s_4\to t_3$ simplifies the integration. We obtain

$$H=-\frac{g^4}{2}v_l K_l(\overleftrightarrow{\lambda})\frac{1}{(4\pi)^d}\int_0^\infty dt_1dt_2dt_3$$
$$\times\int_0^1 dx\int_0^{1-x}dy\frac{\exp[-\tau(t_1+t_2+t_3)]}{[t_1t_2+t_2t_3+t_1t_3]^{d/2+n}}t_1^2$$
$$\times\{2yt_1[xt_1(t_2+t_3)]^n+2t_2[xt_1t_3]^n$$
$$+xt_1[(1-x)t_1(t_2+t_3)+t_2t_3]^n\}. \quad \text{(D14)}$$

The integrations over x and y are again straightforward. In terms of the parameter integrals we find

$$H=-\frac{g^4}{2}v_l K_l(\overleftrightarrow{\lambda})\left\{-\frac{1}{(n+1)}[M^4_{1,0,1}+M^4_{0,1,1}+M^4_{1,1,0}]\right.$$
$$+\frac{1}{(n+1)(n+2)}[2M^8_{0,1,0}(n)+M^7_{2,0,1}(n)+M^7_{1,1,1}(n)]$$
$$+\frac{1}{(n+2)(n+3)}[M^3_{1,0,1}+M^3_{0,1,1}+(n+4)M^3_{1,1,0}]$$
$$\left.+\frac{2}{(n+1)(n+2)(n+3)}[M^6_{1,0,0}(n)+M^7_{2,1,0}(n)]\right\}. \quad \text{(D15)}$$

Finally we obtain

$$H=-\frac{g^4}{2}v_l K_l(\overleftrightarrow{\lambda})\frac{G_\epsilon^2}{\epsilon}\tau^{-\epsilon}\Bigg\{-\frac{1}{(n+1)(n+2)\epsilon}+\frac{4}{(n+1)^2(n+2)^2\epsilon}-\frac{8n-F_2(n+3)+24}{3(n+1)(n+2)(n+3)}-\frac{11}{6(n+1)^2(n+2)^2}+\frac{1}{3(n+1)(n+2)^2(n+3)}+\frac{4n+6}{(n+1)^3(n+2)^3}\Bigg\}. \tag{D16}$$

The diagrams I to L can be treated in a similar manner.

APPENDIX E: PARAMETER INTEGRALS

This Appendix contains a list of the parameter integrals we use in the calculation of the noise exponents. The results stated are obtained by employing the dimensional regularization scheme. The parameter integral M^1 given below was introduced by Breuer and Janssen [37]. The notation M^2 we reserved for a parameter integral we introduced in [20] but which is not used here. For notational briefness we define

$$F_m(n)=\sum_{k=m}^{n}\binom{n}{k}(-1)^k\frac{1}{k-m+1}. \tag{E1}$$

F_m is related to the Digamma function Ψ via

$$F_m(n)=(-1)^{m+1}\frac{n![\Psi(m)-\Psi(n+1)]}{(m-1)!(1-m+n)!}. \tag{E2}$$

The parameter integrals we use in calculating the ψ_l are

$$M^1(a,b,c)=\int_{\mathbf{p},\mathbf{q}}\frac{1}{(a+\mathbf{p}^2)(b+\mathbf{q}^2)[c+(\mathbf{p}+\mathbf{q})^2]}=\frac{1}{(4\pi)^d}\int_0^\infty dt_1dt_2dt_3\frac{\exp[-(at_1+bt_2+ct_3)]}{[t_3t_1+t_3t_2+t_1t_2]^{d/2}}=\frac{G_\epsilon^2}{6\epsilon}\Bigg\{\left(\frac{1}{\epsilon}+\frac{25}{12}\right)(a^{3-\epsilon}+b^{3-\epsilon}+c^{3-\epsilon})-\left(\frac{3}{\epsilon}+\frac{21}{4}\right)[a^{2-\epsilon}(b+c)+b^{2-\epsilon}(a+c)+c^{2-\epsilon}(a+b)]-3abc\Bigg\}, \tag{E3}$$

$$M^3(a,b,c)=\frac{1}{(4\pi)^d}\int_0^\infty dt_1dt_2dt_3\frac{\exp[-(at_1+bt_2+ct_3)]}{[t_3t_1+t_3t_2+t_1t_2]^{d/2-2}}\frac{1}{[t_1+t_2]^3}=\frac{G_\epsilon^2}{2\epsilon}\Bigg\{c^{2-\epsilon}\left(\frac{1}{15\epsilon}+\frac{46}{450}\right)-c^{1-\epsilon}(a+b)\left(\frac{1}{3\epsilon}+\frac{4}{9}\right)+c^{-\epsilon}(a^2+b^2)\left(\frac{2}{3\epsilon}+\frac{13}{18}\right)+c^{-\epsilon}ab\left(\frac{2}{3\epsilon}+\frac{5}{9}\right)\Bigg\}, \tag{E4}$$

$$M^4(a,b,c)=\frac{1}{(4\pi)^d}\int_0^\infty dt_1dt_2dt_3\frac{\exp[-(at_1+bt_2+ct_3)]}{[t_3t_1+t_3t_2+t_1t_2]^{d/2-1}}\frac{t_1t_2}{[t_1+t_2]^3}=\frac{G_\epsilon^2}{2\epsilon}\Bigg\{-c^{2-\epsilon}\left(\frac{2}{15\epsilon}+\frac{107}{450}\right)-c^{1-\epsilon}(a+b)\left(\frac{1}{3\epsilon}+\frac{4}{9}\right)+\frac{1}{3}(a^2+b^2)+\frac{1}{3}ab\Bigg\}, \tag{E5}$$

$$M^5(a,b,c;n)=\frac{1}{(4\pi)^d}\int_0^\infty dt_1dt_2dt_3\frac{\exp[-(at_1+bt_2+ct_3)]}{[t_3t_1+t_3t_2+t_1t_2]^{d/2}}\frac{t_1^n}{[t_1+t_2]^n}=-\frac{G_\epsilon^2}{6\epsilon}\Bigg\{a^{3-\epsilon}\left[-\frac{n+1}{\epsilon}-\frac{25(n+1)}{12}+\frac{1}{2}F_2(n+1)\right]+c^{3-\epsilon}\frac{1}{(n+2)(n+3)}\times\left[-\frac{6}{\epsilon}-\frac{15}{2}+3\Psi(n+2)+3\Psi(2)-6\Psi(n+4)\right]+a^{2-\epsilon}b\left[\frac{3}{\epsilon}+\frac{21}{4}+\frac{3}{2}F_1(n)\right]+a^{2-\epsilon}c\left[\frac{3}{\epsilon}+\frac{27}{4}+\frac{3}{2}F_1(n+1)\right]+c^{2-\epsilon}a\frac{1}{n+2}\left[\frac{6}{\epsilon}+\frac{9}{2}-3\Psi(n+2)+6\Psi(n+3)+3\gamma\right]$$

$$+c^{2-\epsilon}b\frac{1}{(n+1)(n+2)}\left[\frac{6}{\epsilon}+\frac{9}{2}-3\Psi(n+1)-3\Psi(2)+6\Psi(n+3)\right]$$

$$+b^3\frac{1}{2(n-1)n}+b^2a\frac{3}{2n}+b^2c\frac{3}{2n(n+1)}-3abc\frac{1}{n+1}\Bigg\}, \tag{E6}$$

$$M^6(a,b,c;n)=\frac{1}{(4\pi)^d}\int_0^\infty dt_1dt_2dt_3\frac{\exp[-(at_1+bt_2+ct_3)]}{[t_3t_1+t_3t_2+t_1t_2]^{d/2+n}}\frac{t_3^n[t_1+t_2]^n}{t_1}$$

$$=-\frac{G_\epsilon^2}{\epsilon}\Bigg\{c^{1-\epsilon}\left[\frac{(n+2)(n+3)}{12\epsilon}+\frac{n+3}{6\epsilon}+\frac{11(n+2)(n+3)}{72}+\frac{2(n+3)}{9}-\frac{1}{24}+\frac{1}{12}[F_3(n+3)-F_2(n+3)]\right]$$

$$+c^{-\epsilon}a\left[-\frac{n+3}{3\epsilon}-\frac{5(n+3)}{18}+\frac{1}{6}+\frac{1}{6}F_2(n+3)\right]+c^{-\epsilon}b\left[-\frac{2(n+3)}{3\epsilon}-\frac{13(n+3)}{18}+\frac{1}{6}+\frac{1}{3}F_2(n+3)\right]$$

$$+c^{-(1+\epsilon)}b^2\left(\frac{2}{\epsilon}+\frac{3}{2}\right)-\frac{1}{2}c^{-(1+\epsilon)}a^2-c^{-(1+\epsilon)}ab\Bigg\}, \tag{E7}$$

$$M^7(a,b,c;n)=\frac{1}{(4\pi)^d}\int_0^\infty dt_1dt_2dt_3\frac{\exp[-(at_1+bt_2+ct_3)]}{[t_3t_1+t_3t_2+t_1t_2]^{d/2+n}}\frac{t_1^{n+1}t_2^{n+2}}{[t_1+t_2]^3}$$

$$=-\frac{G_\epsilon^2}{6\epsilon}\Bigg\{b^{3-\epsilon}\left[\frac{2}{(n+2)\epsilon}+\frac{1}{(n+2)^2}+\frac{11}{6(n+2)}\right]+a^3\frac{1}{3(n+2)}+c^3\frac{1}{10(n-1)n(n+1)(n+2)}$$

$$+a^2b\frac{1}{2(n+2)}+a^2c\frac{1}{4(n+1)(n+2)}+b^2a\frac{1}{n+2}+b^2c\frac{3}{4(n+1)(n+2)}+c^2a\frac{1}{5n(n+1)(n+2)}$$

$$+c^2b\frac{3}{10n(n+1)(n+2)}+abc\frac{1}{2(n+1)(n+2)}\Bigg\}, \tag{E8}$$

$$M^8(a,b,c;n)=\frac{1}{(4\pi)^d}\int_0^\infty dt_1dt_2dt_3\frac{\exp[-(at_1+bt_2+ct_3)]}{[t_3t_1+t_3t_2+t_1t_2]^{d/2+n}}t_1^nt_2^{n+1}t_3$$

$$=-\frac{G_\epsilon^2}{\epsilon}\Bigg\{b^{1-\epsilon}\left[\frac{2}{(n+1)(n+2)\epsilon}+\frac{2n+3}{(n+1)^2(n+2)^2}+\frac{1}{(n+1)(n+2)}\right]+a\frac{1}{(n+1)(n+2)}+c\frac{1}{n(n+1)(n+2)}\Bigg\}. \tag{E9}$$

In addition to the parameter integrals we use

$$M=\frac{1}{(4\pi)^d}\int_0^\infty dt_1dt_2dt_3\frac{\exp[-\tau(t_1+t_2+t_3)]}{[t_3t_1+t_3t_2+t_1t_2]^{d/2-2}}\frac{t_3}{t_1(t_1+t_2)}$$

$$=\frac{G_\epsilon^2}{\epsilon}\tau^{-\epsilon}\left(\frac{3}{\epsilon}-\frac{1}{2}\right). \tag{E10}$$

APPENDIX F: CONDUCTING DIAGRAMS IN TERMS OF PARAMETER INTEGRALS

Here we list our results for the conducting two-loop diagrams in terms of the parameter integrals given in Appendix E. For notational simplicity, we show only the parts of the diagrams proportional to $v_lK_l(\overleftrightarrow{\lambda})$:

$$C=-\frac{g^4}{2}v_lK_l(\overleftrightarrow{\lambda})\Bigg\{\frac{2}{(n+1)(n+2)}[M^8_{1,0,0}(n)-2M^7_{2,0,1}(n)$$

$$-4M^7_{1,1,1}(n)-2M^7_{0,2,1}(n)]+\frac{4}{(n+1)(n+2)(n+3)}$$

$$\times[M+M^3_{2,0,0}+M^3_{1,1,0}-M^6_{1,0,0}(n)-M^6_{0,1,0}(n)$$

$$-M^7_{3,0,0}(n)-M^7_{2,1,0}(n)]\Bigg\}, \tag{F1}$$

$$D=-\frac{g^4}{2}v_lK_l(\overleftrightarrow{\lambda})\Bigg\{\frac{n^2+3n+6}{2(n+1)(n+2)}M^1_{2,1,0}$$

$$+\frac{2}{(n+1)(n+2)}M^1_{1,1,1}\Bigg\}, \tag{F2}$$

$$E=-\frac{g^4}{2}v_l K_l(\overleftrightarrow{\lambda})\Bigg\{-\frac{4}{(n+1)(n+2)}M^5_{2,1,0}(n)+\frac{8}{(n+1)(n+2)(n+3)}[M^1_{3,0,0}+3M^1_{2,1,0}-M^5_{3,0,0}(n)]\Bigg\}, \tag{F3}$$

$$F=-\frac{g^4}{2}v_l K_l(\overleftrightarrow{\lambda})\{M^1_{2,1,0}+M^1_{1,1,1}\}, \tag{F4}$$

$$G=-\frac{g^4}{2}v_l K_l(\overleftrightarrow{\lambda})M^1_{2,1,0}, \tag{F5}$$

$$H=-\frac{g^4}{2}v_l K_l(\overleftrightarrow{\lambda})\Bigg\{-\frac{1}{(n+1)}[M^4_{1,0,1}+M^4_{0,1,1}+M^4_{1,1,0}]+\frac{1}{(n+1)(n+2)}[2M^8_{0,1,0}(n)+M^7_{2,0,1}(n)+M^7_{1,1,1}(n)]+\frac{1}{(n+2)(n+3)}[M^3_{1,0,1}+M^3_{0,1,1}+(n+4)M^3_{1,1,0}]+\frac{2}{(n+1)(n+2)(n+3)}[M^6_{1,0,0}(n)+M^7_{2,1,0}(n)]\Bigg\}, \tag{F6}$$

$$I=-\frac{g^4}{2}v_l K_l(\overleftrightarrow{\lambda})\Bigg\{\frac{1}{3}M^1_{3,0,0}+M^5_{0,1,2}(n)\Bigg\}, \tag{F7}$$

$$J=-\frac{g^4}{2}v_l K_l(\overleftrightarrow{\lambda})\Bigg\{\frac{2}{(n+1)(n+2)}M^5_{2,1,0}(n)+\frac{1}{(n+1)(n+2)(n+3)}[4M^5_{3,0,0}(n)+(n-1)M^1_{3,0,0}+3(n-1)M^1_{2,1,0}]\Bigg\}, \tag{F8}$$

$$K=-\frac{g^4}{2}v_l K_l(\overleftrightarrow{\lambda})\Bigg\{\frac{1}{3}M^1_{3,0,0}+\frac{1}{2}M^1_{2,1,0}\Bigg\}, \tag{F9}$$

$$L=-\frac{g^4}{2}v_l K_l(\overleftrightarrow{\lambda})\frac{1}{6}M^1_{3,0,0}. \tag{F10}$$

APPENDIX G: RELATION TO THE BACKBONE AND THE RED BOND DIMENSION

From Eq. (2.21) it is evident that only those bonds with $I_b=I$ contribute to $C_R^{(\infty)}$. Consequently, ψ_∞ is related to the fractal dimension $d_{\rm red}$ of the singly connected (red) bonds via $d_{\rm red}=\psi_\infty/\nu$. Coniglio [38,39] proved that $d_{\rm red}=1/\nu$, which in turn leads to $\psi_\infty=1$. As mentioned above, our result for ψ_l matches this consistency requirement.

Another trivial consequence of Eq. (2.21) is that $C_R^{(0)}$ is proportional to the average number of bonds (the mass) of the backbone. Hence ψ_0 is related to the backbone dimension D_B by

$$\psi_0=\nu D_B. \tag{G1}$$

This relation can also be obtained on the level of Feynman diagrams. Reconsider the definition of the noise cumulants for Feynman diagrams Eq. (3.9). In the limit $l\to 0$ the noise cumulant reduces to the sum of Schwinger parameters of conducting propagators,

$$C^{(0)}(\{s_i\})=\sum_i s_i. \tag{G2}$$

Now we take a short detour to our renormalized field theory of diluted networks in which the occupied bonds obey a generalized Ohm's law $V\sim I^r$ [21,22]. In these networks, the nonlinear resistance $R_r(x,x')$ averaged subject to x and x' being on the same cluster,

$$M_r(x,x')=\langle\chi(x,x')R_r(x,x')\rangle_C/\langle\chi(x,x')\rangle_C, \tag{G3}$$

obeys at criticality

$$M_r(x,x')=|x-x'|^{\phi_r/\nu}. \tag{G4}$$

In analogy to $R(\{s_i\})$ we introduced the notion of the nonlinear resistance $R_r(\{s_i\})$ of Feynman diagrams. In the limit $r\to -1^+$ we found

$$R_{-1}(\{s_i\})=\sum_i s_i. \tag{G5}$$

Hence we can identify $C^{(0)}(\{s_i\})$ and $R_{-1}(\{s_i\})$. This leads to the conclusion that $\psi_0=\phi_{-1}$. ϕ_{-1} is related to the fractal dimension D_B of the backbone via $\phi_{-1}=\nu D_B$, and hence we obtain once more Eq. (G1). Equation (G1) provides another consistency check for our result (3.38), which is indeed fulfilled. Moreover, Eq. (G1) can be used to calculate ψ_0 to third order in ϵ from our three-loop result for D_B [21,22],

$$D_B=2+\frac{1}{21}\epsilon-\frac{172}{9261}\epsilon^2-2\frac{74\,639-22\,680\zeta(3)}{4\,084\,101}\epsilon^3+O(\epsilon^4). \tag{G6}$$

We obtain

$$\psi_0=1+\frac{1}{7}\epsilon+\frac{313}{12\,348}\epsilon^2-\frac{166\,823+417\,312\zeta(3)}{21\,781\,872}\epsilon^3+O(\epsilon^4). \tag{G7}$$

[1] For reviews on percolation, see, e.g., A. Bunde and S. Havlin, *Fractals and Disordered Systems* (Springer, Berlin, 1991); D. Stauffer and A. Aharony, *Introduction to Percolation Theory* (Taylor and Francis, London, 1992); B. D. Hughes, *Random Walks and Random Environments* (Clarendon, Oxford, 1995).

[2] For general aspects of multifractals, see C. J. C. Evertsz and B. B. Mandelbrot, in *Chaos and Fractals: New Frontiers of Science*, edited by H. O. Peitgen, H. Jurgens, and D. Saupe (Springer, New York, 1992), p. 849; For a review in the context of RRN's, see A. Hansen, in *Statistical Models for the Fracture of Disordered Media*, edited by H. J. Herrmann and S. Roux (Elsevier, Amsterdam, 1990), p. 115.

[3] B.B. Mandelbrot, J. Fluid Mech. **62**, 331 (1974); U. Frisch and G. Parisi, in *Turbulence and Predictability in Geophysical Fluid Dynamics and Climate Dynamics*, Proceedings of the International School of Physics ''Enrico Fermi,'' Course LXXXVIII, Varenna, 1983, edited by M. Ghil (North-Holland, New York, 1985), p. 84; R. Benzi, G. Paladin, G. Parisi, and A. Vulpiani, J. Phys. A **18**, 3521 (1984).

[4] M.E. Cates and T.A. Witten, Phys. Rev. A **35**, 1809 (1987).

[5] F. Wegner, Nucl. Phys. B **280**, 193 (1987); C. Castellani and L. Peliti, J. Phys. A **19**, L429 (1986).

[6] D. Gersappe, J.M. Deutsch, and M. Olvera de la Cruz, Phys. Rev. Lett. **66**, 731 (1991).

[7] A.W.W. Ludwig, Nucl. Phys. B **285**, 97 (1987); **330**, 639 (1990).

[8] T.C. Halsey, M.H. Jensen, L.P. Kadanoff, I. Procaccia, and B. Shraiman, Phys. Rev. A **33**, 1141 (1986).

[9] P.Ch. Ivanov *et al.*, Nature (London) **399**, 461 (1999).

[10] L. de Arcangelis, S. Redner, and A. Coniglio, Phys. Rev. B **34**, 4656 (1986).

[11] R. Rammal, C. Tannous, and A.-M.S. Tremblay, Phys. Rev. A **31**, 2662 (1985); R. Rammal, C. Tannous, P. Brenton, and A.-M.S. Tremblay, Phys. Rev. Lett. **54**, 1718 (1985).

[12] R.M. Cohn, Am. Math. Soc. **1**, 316 (1950).

[13] L. de Arcangelis, S. Redner, and A. Coniglio, Phys. Rev. B **31**, 4725 (1985).

[14] Y. Park, A.B. Harris, and T.C. Lubensky, Phys. Rev. B **35**, 5048 (1987).

[15] M.J. Stephen, Phys. Rev. B **17**, 4444 (1978).

[16] B. Duplantier and W.W. Ludwig, Phys. Rev. Lett. **66**, 247 (1991).

[17] B. Fourcade and A.-M.S. Tremblay, Phys. Rev. E **51**, 4095 (1995).

[18] G.G. Batrouni, A. Hansen, and B. Larson, Phys. Rev. E **53**, 2292 (1996).

[19] M. Barthélémy, S.V. Buldyrev, S. Havlin, and H.E. Stanley, Phys. Rev. E **61**, R3283 (2000).

[20] O. Stenull, H.K. Janssen, and K. Oerding, Phys. Rev. E **59**, 4919 (1999).

[21] H.K. Janssen, O. Stenull, and K. Oerding, Phys. Rev. E **59**, R6239 (1999).

[22] H.K. Janssen and O. Stenull, Phys. Rev. E **61**, 4821 (2000).

[23] O. Stenull and H.K. Janssen, Europhys. Lett. **51**, 539 (2000).

[24] See, e.g., R.K.P. Zia and D.J. Wallace, J. Phys. A **8**, 1495 (1975).

[25] M. E. Fisher, in *Renormalization Group in Critical Phenomena and Quantum Field Theory—Proceedings of a Conference*, edited by J. D. Gunton and M. S. Green (Temple University Press, Philadelphia, 1974).

[26] D.J. Amit and L. Peliti, Ann. Phys. (N.Y.) **140**, 207 (1982).

[27] H. W. Diehl, in *Phase Transitions and Critical Phenomena*, edited by C. Domb and J. L. Lebowitz (Academic Press, London, 1986), Vol. 10, p. 171.

[28] See, e.g., D. J. Amit, *Field Theory, the Renormalization Group, and Critical Phenomena* (World Scientific, Singapore, 1984); J. Zinn-Justin, *Quantum Field Theory and Critical Phenomena* (Clarendon, Oxford, 1989).

[29] O.F. de Alcantara Bonfim, J.E. Kirkham, and A.J. McKane, J. Phys. A **13**, L247 (1980); **14**, 2391 (1981).

[30] T.C. Lubensky and J. Wang, Phys. Rev. B **33**, 4998 (1985).

[31] See, e.g., *Handbook of Mathematical Functions*, edited by M. Abramowitz and I. A. Stegun (Dover Publications, New York, 1965).

[32] R. Blumenfeld, Y. Meir, A. Aharony, and A.B. Harris, Phys. Rev. B **35**, 3524 (1987).

[33] C. Moukarzel, Int. J. Mod. Phys. C **8**, 887 (1998).

[34] P. Grassberger, Physica A **262**, 251 (1999).

[35] O. Stenull and H. K. Janssen (unpublished).

[36] See, e.g., I. S. Gradshteyn and I. M. Ryzhik, *Table of Integrals, Series, and Products*, 4th ed. (Academic Press, New York, 1980).

[37] N. Breuer and H.K. Janssen, Z. Phys. B: Condens. Matter **41**, 55 (1981).

[38] A. Coniglio, Phys. Rev. Lett. **46**, 250 (1981).

[39] A. Coniglio, J. Phys. A **15**, 3829 (1982).

[40] C. von Ferber and Y. Holovatch, Europhys. Lett. **39**, 31 (1997); in *Renormalization Group 96, Dubna*, edited by D. V. Shirkov, D. J. Kazakov, and V. B. Priezzhev (World Scientific, Singapore, 1997); Phys. Rev. E **59**, 6914 (1999).